Journal of New Developments in Chemistry

Open Access - Peer-Reviewed - ISSN 2377-2549

Portico Archived | Crossref DOI | CC BY 4.0 Licensed

Research Article

FT-IR, FT-Raman, Homo-Lumo and UV-Visible Spectral Analysis of E-(N′-(1H-INDOL-3YL) Methylene Isonicotinohydrazide)

D.Sumathi [a], H. Saleem [a*], A. Nathiya [a], N.RameshBabu [b], D.Usha [c]

[a] Department of Physics, Annamalai University, Annamalainagar-608 002, Tamil Nadu, India

[b] Department of Physics, MIET Engineering College, Tiruchirappalli – 620 007, Tamil Nadu, India

[c] Department of Physics, Women's Christian college, Nagercoil – 629 001, Tamil Nadu, India

*** Correspondence:** N.RameshBabu, Department of Physics, MIET Engineering College, Tiruchirappalli – 620 007, Tamil Nadu, India.

Published citation: D.Sumathi, H. Saleem, A. Nathiya, N.RameshBabu, D.Usha (2017) **FT-IR, FT-Raman, Homo-Lumo and UV-Visible Spectral Analysis of E-(N′-(1H-INDOL-3YL) Methylene Isonicotinohydrazide)**. *Journal of New Developments in Chemistry* - 1(3):1-36. https://doi.org/10.14302/issn.2377-2549.jndc-17-1459

Article DOI: 10.14302/issn.2377-2549.jndc-17-1459

Abstract

A combined experimental and theoretical study on molecular and vibrational structure of E-[N′-(1H-indol-3yl) methylene isonicotinohydrazide] (ICINH) had been carried out. The FTIR, FT-Raman and UV-Vis spectra of ICINH were recorded in the solid phase. The optimized geometry was calculated by the B3LYP method with 6-311++G(d,p) level of basis set. The harmonic vibrational frequencies, IR intensities and Raman scattering activities of the title compound were calculated at the same level of theory. The scaled theoretical wavenumber showed very good agreement with the experimental values. The mulliken charges and thermodynamic functions of the ICINH were also performed at the same level of theory. NLO and a study on the electronic properties such as excitation energies and wavelength were performed by TD-DFT approach. HOMO–LUMO energy gap was also calculated and interpreted.

Keywords:
ICINH; DFT; NLO; NBO; MEP

Article Information	
Academic Editor	Dr. Ashish Kumar, Associate Professor and HOD -Department of Chemistry, Lovely Professional University Phagwara
Received Date	14 February 2017
Accepted Date	25 March 2017

Article Information (continued)

Published Date	22 May 2017
Online	22 May 2017
Publication	Volume 1; Issue 3; Pages 1–36
Copyright	© 2017 D Sumathi, et al
License	This is an open-access article distributed under the terms of the Creative Commons Attribution License, which permits unrestricted use, distribution, and reproduction in any medium, provided the original author and source are credited. https://creativecommons.org/licenses/by/4.0/

Introduction

Indole is an aromatic heterocyclic organic compound with a bicyclic structure. It consists of a six-membered benzene ring fused with five-member nitrogen containing pyrrole ring. It is of interest as it can be compared with tryptophane residue [1]. The derivative of indole is present in both animals and plants. The most important compound of this group is tryptophan, an essential amino acid in the human diet, which is a 3-substituted indole [2]. Another important indole derivative is the indole-3-acetic acid, a phytohormone, coordinating several growth processes of plants [3]. The biological activity of the indole derivatives is in connection with the nature of substitution in position 3, on the pyrrole ring [4]. Indole derivatives have an important role through individual biological functions. It is present in the side chain of amino acid tryptophan. The chemical and spectroscopic properties of indole derivatives have been the subject of many experimental and theoretical investigations [5], [6], [7]. The indole tryptamine if one of the biogenic monoamines would play anti-tumor effects by either inhibiting cancer cell proliferation or stimulating the anti-cancer immunity [8]. DFT method has become an efficient tool in the prediction of molecular structure of organic molecules and in evaluating various molecular properties like conjugation, hydrogen bonding, vibrational frequencies and IR & Raman activities of the bioactive molecule [9], [10], [11], [12], [13].

The new Donor-π-Acceptor type dyes $D_{1\text{-}3}$ carrying 3-(1-hexyl-1H-indol-3-yl)-2-(thiophen-2-yl) acrylonitrile as backbone with three different acceptor units were designed and synthesized by Babu, [14], using sensitizers for solar cell application. The new dyes were characterized by various spectral and elemental analyses. Their optical and electrochemical properties were investigated using spectrophotometry and cyclic voltammetry, respectively. The DFT study was carried out to investigate their Frontier MO energy states. The above study reveals that the dye carrying 4-aminobenzoic acid as an acceptor showed the highest photovoltaic efficiency among the three dyes. This can be attributed to the longer electron lifetime and lower recombination rates. Additionally, a single crystal XRD study confirms the structure of a key intermediate.

The stability of the *syn* and *anti* structures of the non-steroidal anti-inflammatory drug indomethacin was investigated by Hassan et al., [15], using the DFT/B3LYP and *ab initio* MP2 calculations with the 6-311G(d,p) basis set. The molecule indomethacin was predicted at the DFT and MP2 levels of calculation to have the *syn* ($C_1N_7C_{10}C_{18}$ ~ 40˚) form being about 1.7 and 1.5 kcal/mol, respectively, lower in energy than the *anti* ($C_1N_7C_{10}C_{18}$ ~ 140˚) structure. The calculated CNCC torsional angles for the chlorobenzene and indole rings *syn-anti* conformational interconversion were in a good qualitative agreement with the reported XRD angles ($C_1N_7C_{10}C_{18}$ ~ 29 and 155˚) for the syn and anti conformers, respectively. Indomethacin was estimated from the calculated Gibb's free energies to have an equilibrium mixture of 95% *syn* and 5% *anti* structures at 298.15 K. The vibrational wavenumbers were calculated at the same level of theory. The complete vibrational assignments were provided on the basis of theoretical and NCA combined with experimental IR and Raman data of the molecule. The analysis of the observed spectra supported the presence of indomethacin in only one conformation at room temperature.

The (E)-2-(2-hydroxybenzylidenamino)-3-(1H-indol-3yl) propionic acid was synthesized by Saleem et al., [7]. To identify the stable structure, the theoretical conformational analysis was performed. The optimized molecular bond parameters were calculated using B3LYP/6-31G(d,p) basis set. The hyper-

conjugative interaction energy ($E^{(2)}$) and EDs of donor (i) and acceptor (j) bonds were calculated using NBO analysis. The dipole moment (μ) and first order hyperpolarizability (β_0) were calculated. The band gap energy was analyzed by UV–Vis recorded spectra and compared with theoretical band gap (TD-DFT/B3LYP/6-31G(d,p)) value. The intra-molecular hydrogen bonding interaction was studied between nitrogen and hydroxyl hydrogen (N-H---O).

The molecular structure, complete vibrational spectra and the quantum mechanical calculations of the title compound were not yet reported. Therefore, the vibrational spectrum and the quantum mechanical calculations for the title compound in the ground state by the DFT method with the standard 6-311++G(d,p) level of basis set were reported. Electronic absorption spectra of the title compound were predicted by using TD-DFT method. The excitation energies, wavelength and oscillator strengths were obtained at the same level of theory. Besides the molecular parameters, dipole moments, NLO, thermodynamic properties, linear polarizability and first hyperpolarizability were calculated. The results obtained from theoretical calculations and experiments were compared.

Experimental Details

Synthesis Procedure

1H-indole-3-carbaldehyde (1.45 g, 0.01 mol) and isonicotinic acid hydrazide (1.37 g, 0.01 mol) were added to ethanol (10 ml) and stirred for an hour in the presence of hydrochloric acid to form a white precipitate. The precipitate was washed with sodium bicarbonate solution and filtered and again washed with petroleum ether (40–60%) and dried in air. The compound was recrystallized from absolute ethanol.

Results and Discussion

Molecular Geometry

The optimized structural parameters of E-[N′-(1H-indol-3-ylmethylene) isonicotinohydrazide] are calculated using B3LYP/6-311++G(d,p) basis set and listed in Table 1. The optimized structure is shown in Figure 1. The title molecule consists of pyridine and indole rings fused by hydrazone linkage. In ICINH, the hydrazone linkage plays an important role. For the carbonyl (C_{21}=O_{29}) bond length in hydrazone link is calculated about 1.223Å using DFT and corresponding X-ray data value is 1.236Å. The bond length of N_{18}-N_{19} is acted as bridge between the phenyl and pyridine ring and its bond length is calculated using DFT calculation at 1.368Å, while the corresponding X-rays value is 1.392Å. Similarly, the C_{21}-N_{19}/C_{16}=N_{18} bond lengths are calculated as: 1.384: DFT; 1.330Å: X-rays data/1.288: DFT; 1.278Å: X-rays data, respectively. In the present study, the average value of C-C bond lengths in indole ring is 1.403Å (DFT). Bikas et al., [16], observed the bond angle of O-C-C at 120.6˚, which was consistent

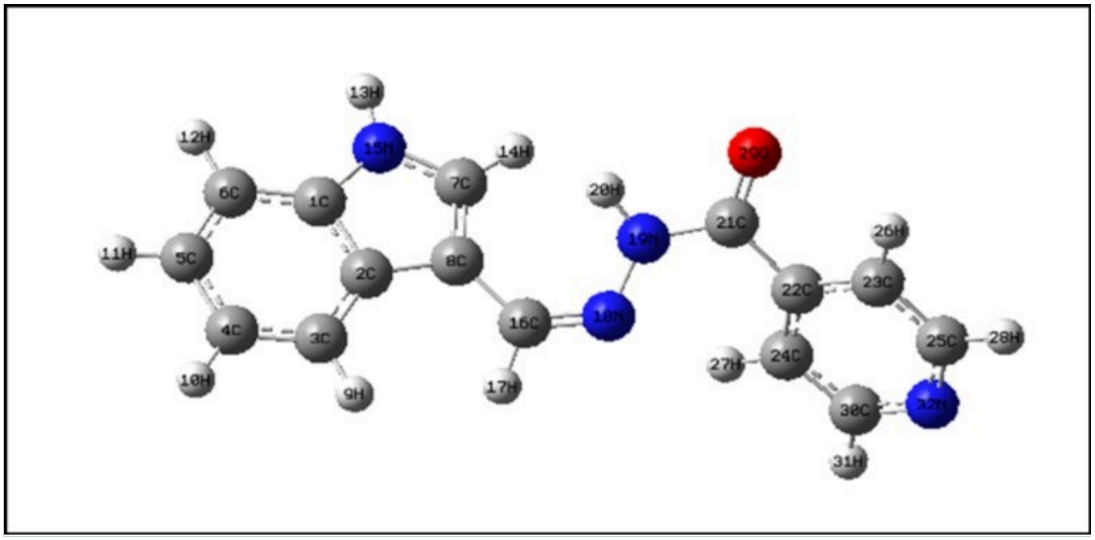


Figure 1. The optimized molecular structure of ICINH

 DOI: 10.14302/issn.2377-2549.jndc-17-1459

with calculated value 121.49˚ (O_{29}-C_{21}-C_{22}) and its corresponding DFT value is positively deviated (~ 1˚) from the calculated value. The dihedral angles are also calculated and listed in Table 1.

Table 1. The optimized bond parameters of ICINH using B3LYP/6-311++G(d,p) basis set

Bond Parameters	B3LYP/6-311++G(d,p)	XRD[a]
Bond Lengths (Å)		
C_1-C_2	1.416	
C_1-C_6	1.396	
C_1-N_{15}	1.383	1.347
C_2-C_3	1.404	
C_2-C_8	1.451	1.445
C_3-C_4	1.387	
C_3-H_9	1.084	
C_4-C_5	1.408	
C_4-H_{10}	1.084	
C_5-C_6	1.388	
C_5-H_{11}	1.084	
C_6-H_{12}	1.084	
C_7-C_8	1.385	
C_7-H_{14}	1.078	
C_7-N_{15}	1.372	
C_8-C_{16}	1.455	1.437
H_{13}-N_{15}	1.007	
C_{16}-H_{17}	1.087	
C_{16}-N_{18}	1.288	1.278
N_{18}-N_{19}	1.368	1.392
N_{19}-H_{20}	1.019	
N_{19}-C_{21}	1.384	1.33
C_{21}-C_{22}	1.496	1.495
C_{21}-O_{29}	1.223	1.236
C_{22}-C_{23}	1.398	
C_{22}-C_{24}	1.401	
C_{23}-C_{25}	1.388	
C_{23}-H_{26}	1.083	

 DOI: 10.14302/issn.2377-2549.jndc-17-1459

Table 1 (continued)

Bond Parameters	B3LYP/6-311++G(d,p)	XRD[a]
C_{24}-H_{27}	1.082	
C_{24}-N_{31}	1.335	
C_{25}-C_{28}	1.394	
C_{25}-H_{29}	1.084	
C_{28}-H_{30}	1.0867	
C_{28}-N_{31}	1.336	
Bond Angles (°)		
C_2-C_1-C_6	122.55	
C_2-C_1-N_{15}	107.12	109.56
C_6-C_1-N_{15}	130.34	
C_1-C_2-C_3	118.87	
C_1-C_2-C_8	107.31	
C_3-C_2-C_8	133.81	
C_2-C_3-C_4	118.90	
C_2-C_3-H_9	120.86	
C_4-C_3-H_9	120.24	
C_3-C_4-C_5	121.19	
C_3-C_4-H_{10}	119.60	
C_5-C_4-H_{10}	119.20	
C_4-C_5-C_6	121.18	
C_4-C_5-H_{11}	119.40	
C_6-C_5-H_{11}	119.42	
C_1-C_6-C_5	117.31	
C_1-C_6-H_{12}	121.52	
C_5-C_6-H_{12}	121.17	
C_8-C_7-H_{14}	130.27	
C_8-C_7-N_{15}	109.75	
H_{14}-C_7-N_{15}	119.85	123.30
C_2-C_8-C_7	106.01	
C_2-C_8-C_{16}	123.89	130.50
C_7-C_8-C_{16}	129.95	

 DOI: 10.14302/issn.2377-2549.jndc-17-1459

Table 1 (continued)

Bond Parameters	B3LYP/6-311++G(d,p)	XRD[a]
C_1-N_{15}-C_7	109.81	
C_1-N_{15}-H_{13}	125.49	
C_7-N_{15}-H_{13}	124.69	
C_8-C_{16}-H_{17}	115.93	
C_8-C_{16}-N_{18}	130.93	
H_{17}-C_{16}-N_{18}	113.14	
C_{16}-N_{18}-N_{19}	117.96	113.29
N_{18}-N_{19}-H_{20}	119.23	
N_{18}-N_{19}-C_{21}	123.39	120.33
H_{20}-N_{19}-C_{21}	112.73	
N_{19}-C_{21}-C_{22}	119.89	114.64
N_{19}-C_{21}-O_{29}	118.60	124.70
C_{22}-C_{21}-O_{29}	121.49	120.60
C_{21}-C_{22}-C_{23}	117.13	
C_{21}-C_{22}-C_{24}	124.87	
C_{23}-C_{22}-C_{24}	117.85	
C_{22}-C_{23}-C_{25}	119.05	
C_{22}-C_{23}-H_{26}	119.22	
C_{25}-C_{23}-H_{26}	121.73	
C_{22}-C_{24}-H_{27}	120.51	
C_{22}-C_{24}-N_{31}	123.46	
H_{27}-C_{24}-N_{31}	116.03	
C_{23}-C_{25}-C_{28}	118.39	
C_{23}-C_{25}-H_{29}	121.19	
C_{28}-C_{25}-H_{29}	120.41	
C_{25}-C_{28}-H_{30}	120.46	
C_{25}-C_{28}-N_{31}	123.50	
H_{30}-C_{28}-N_{31}	116.05	
C_{24}-N_{31}-C_{28}	117.73	
Dihedral Angles (°)		
C_6-C_1-C_2-C_3	-0.05	

 DOI: 10.14302/issn.2377-2549.jndc-17-1459

Table 1 (continued)

Bond Parameters	B3LYP/6-311++G(d,p)	XRD[a]
C_6-C_1-C_2-C_8	-179.54	
N_{15}-C_1-C_2-C_3	179.79	
N_{15}-C_1-C_2-C_8	0.29	
C_2-C_1-C_6-C_5	-0.29	
C_2-C_1-C_6-H_{12}	179.72	
N_{15}-C_1-C_6-C_5	179.92	
N_{15}-C_1-C_6-H_{12}	-0.07	
C_2-C_1-N_{15}-C_7	-0.26	
C_2-C_1-N_{15}-H_{13}	179.33	
C_6-C_1-N_{15}-C_7	179.56	
C_6-C_1-N_{15}-H_{13}	-0.85	
C_1-C_2-C_3-C_4	0.41	
C_1-C_2-C_3-H_9	-179.24	
C_8-C_2-C_3-C_4	179.74	
C_8-C_2-C_3-H_9	0.09	
C_1-C_2-C_8-C_7	-0.22	
C_1-C_2-C_8-C_{16}	-176.16	
C_3-C_2-C_8-C_7	-179.61	
C_3-C_2-C_8-C_{16}	4.45	
C_2-C_3-C_4-C_5	-0.44	
C_2-C_3-C_4-H_{10}	179.88	
H_9-C_3-C_4-C_5	179.21	
H_9-C_3-C_4-H_{10}	-0.47	
C_3-C_4-C_5-C_6	0.11	
C_3-C_4-C_5-H_{11}	-179.77	
H_{10}-C_4-C_5-C_6	179.78	
H_{10}-C_4-C_5-H_{11}	-0.09	
C_4-C_5-C_6-C_1	0.26	
C_4-C_5-C_6-H_{12}	-179.75	
H_{11}-C_5-C_6-C_1	-179.87	
H_{11}-C_5-C_6-H_{12}	0.12	

 DOI: 10.14302/issn.2377-2549.jndc-17-1459

Table 1 (continued)

Bond Parameters	B3LYP/6-311++G(d,p)	XRD[a]
H_{14}-C_7-C_8-C_2	-175.75	
H_{14}-C_7-C_8-C_{16}	-0.14	
N_{15}-C_7-C_8-C_2	0.06	
N_{15}-C_7-C_8-C_{16}	175.67	
C_8-C_7-N_{15}-C_1	0.12	
C_8-C_7-N_{15}-H_{13}	-179.48	
H_{14}-C_7-N_{15}-C_1	176.44	
H_{14}-C_7-N_{15}-H_{13}	-3.16	
C_2-C_8-C_{16}-H_{17}	20.44	
C_2-C_8-C_{16}-N_{18}	-158.81	
C_8-C_{16}-N_{18}-N_{19}	-154.47	
H_{17}-C_{16}-N_{18}-N_{19}	26.29	
C_{16}-N_{18}-N_{19}-H_{20}	2.17	
C_{16}-N_{18}-N_{19}-C_{21}	-177.10	
N_{18}-N_{19}-C_{21}-C_{22}	21.38	
N_{18}-N_{19}-C_{21}-O_{32}	175.42	
H_{20}-N_{19}-C_{21}-C_{22}	21.29	
H_{20}-N_{19}-C_{21}-O_{32}	-160.76	
N_{19}-N_{21}-C_{22}-C_{23}	176.81	
N_{19}-N_{21}-C_{22}-C_{24}	-5.23	
O_{32}-C_{21}-C_{22}-C_{23}	-156.35	
O_{32}-C_{21}-C_{22}-C_{24}	28.10	
C_{21}-C_{22}-C_{23}-C_{25}	25.76	
C_{21}-C_{22}-C_{23}-H_{26}	-149.79	
C_{24}-C_{22}-C_{23}-C_{25}	-177.41	
C_{24}-C_{22}-C_{23}-H_{26}	2.29	
C_{21}-C_{22}-C_{24}-H_{27}	-1.54	
C_{21}-C_{22}-C_{24}-N_{31}	178.16	
C_{23}-C_{22}-C_{24}-H_{27}	-3.35	
C_{23}-C_{22}-C_{24}-N_{31}	175.99	
C_{22}-C_{23}-C_{25}-C_{28}	-178.87	

Table 1 (continued)

Bond Parameters	B3LYP/6-311++G(d,p)	XRD[a]
C_{22}-C_{23}-C_{25}-H_{29}	0.47	
H_{26}-C_{23}-C_{25}-C_{28}	1.25	
H_{26}-C_{23}-C_{25}-H_{29}	-179.20	
C_{22}-C_{24}-N_{31}-C_{28}	-178.45	
H_{27}-C_{24}-N_{31}-C_{28}	1.10	
C_{23}-C_{25}-C_{28}-H_{30}	0.92	
C_{23}-C_{25}-C_{28}-N_{31}	-179.72	
H_{29}-C_{25}-C_{28}-H_{30}	179.80	
H_{29}-C_{25}-C_{28}-N_{31}	0.18	
C_{25}-C_{28}-N_{31}-C_{24}	0.25	
H_{30}-C_{28}-N_{31}-C_{24}	-179.37	

[a] Zuo-Liang Jing, Wen-Wen, Cheng, Xin Chen and Yu Ming, 200-(1H-Indol-3-ylmethylene)isonicotinohydrazide ethanol solvate, Acta Cryst. (2006). E62, o1360–o1361.

Vibrational Assignments

The harmonic vibrational frequencies were calculated using B3LYP/6-311++G(d,p) basis set. The title molecule belongs to C_1 point group symmetry and its 90 vibrational normal modes of the same symmetry species are listed in Table 2.1. The internal and symmetry coordinates of ICINH are listed in Table 2.1 and Table 2.2, respectively. The percentage of PED obtained from MOLVIB program package was used for assigning vibrational peaks. The exclusion of anharmonicity factor and the level of basis set used, certain theoretical frequencies are not matched with that of the experimental values. Hence linear scaling procedure is adopted to scale down the frequency values. In this study, we have followed a scaling factor of 0.968 for DFT [17]. The observed FT-IR, FT-Raman and simulated spectra of ICINH are shown in Figure 2 and Figure 3, respectively.

Table 2.1. Possible internal co-ordinates of ICINH

S.No	Type	Fragment type	Definition
1-8	C-C	Double ring	C_1-C_2, C_2-C_3, C_3-C_4, C_4-C_5, C_5-C_6, C_6-C_1, C_2-C_8, C_7-C_8
9,10	C-N		C_1-N_{15}, C_7-N_{15}
11-15	C-H		C_3-H_9, C_4-H_{10}, C_5-H_{11}, C_6-H_{12}, C_7-H_{14}
16	N-H		N_{15}-H_{13}
17-20	C-C	Pyridine ring	C_{22}-C_{23}, C_{22}-C_{24}, C_{23}-C_{25}, C_{25}-C_{28}
21,22	C-N		C_{24}-N_{31}, C_{28}-N_{31}
23-26	C-H		C_{23}-H_{26}, C_{24}-H_{27}, C_{25}-H_{29}, C_{28}-H_{30}

DOI: 10.14302/issn.2377-2549.jndc-17-1459

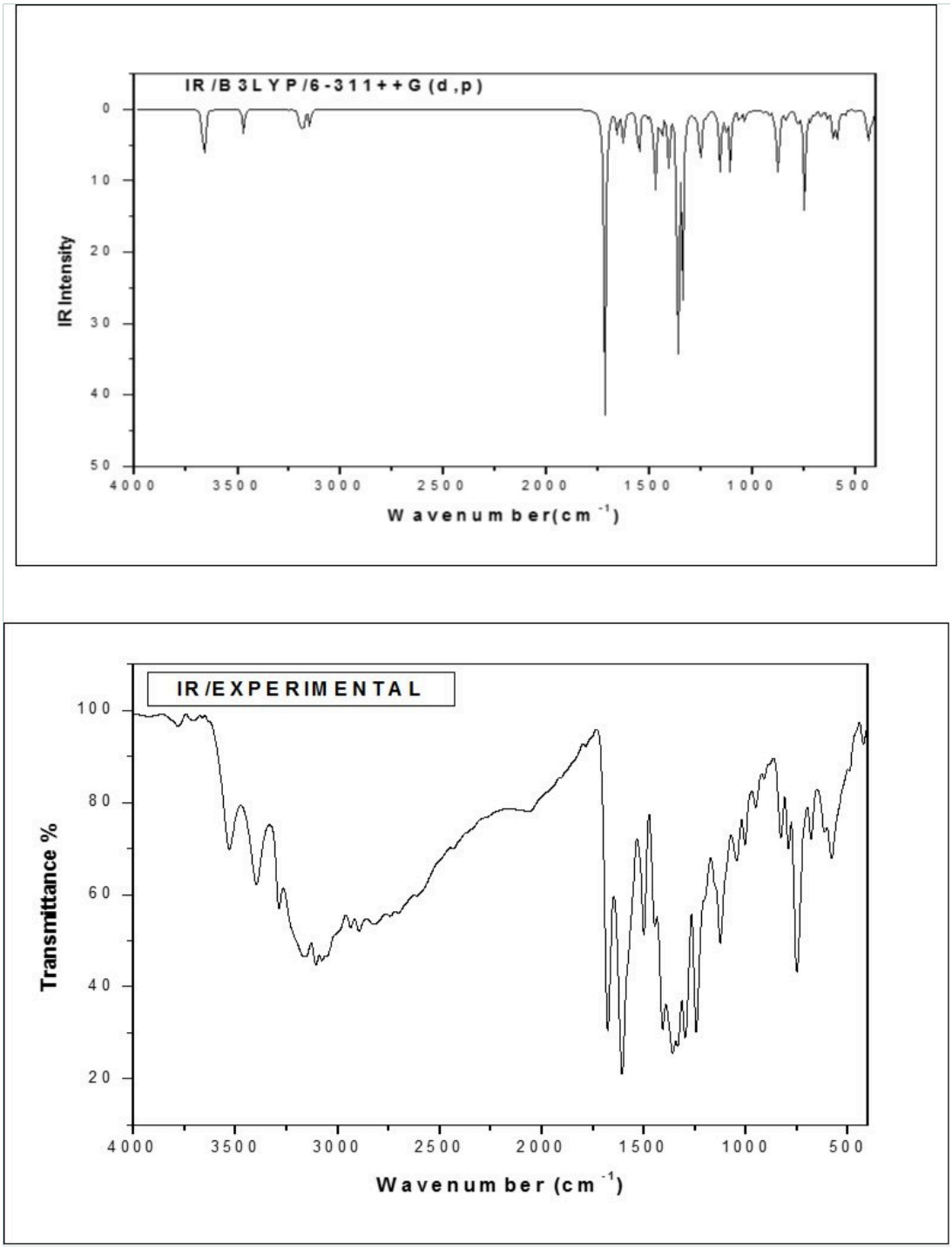


Figure 2. The combined theoretical and experimental FT-IR spectra of ICINH

DOI: 10.14302/issn.2377-2549.jndc-17-1459

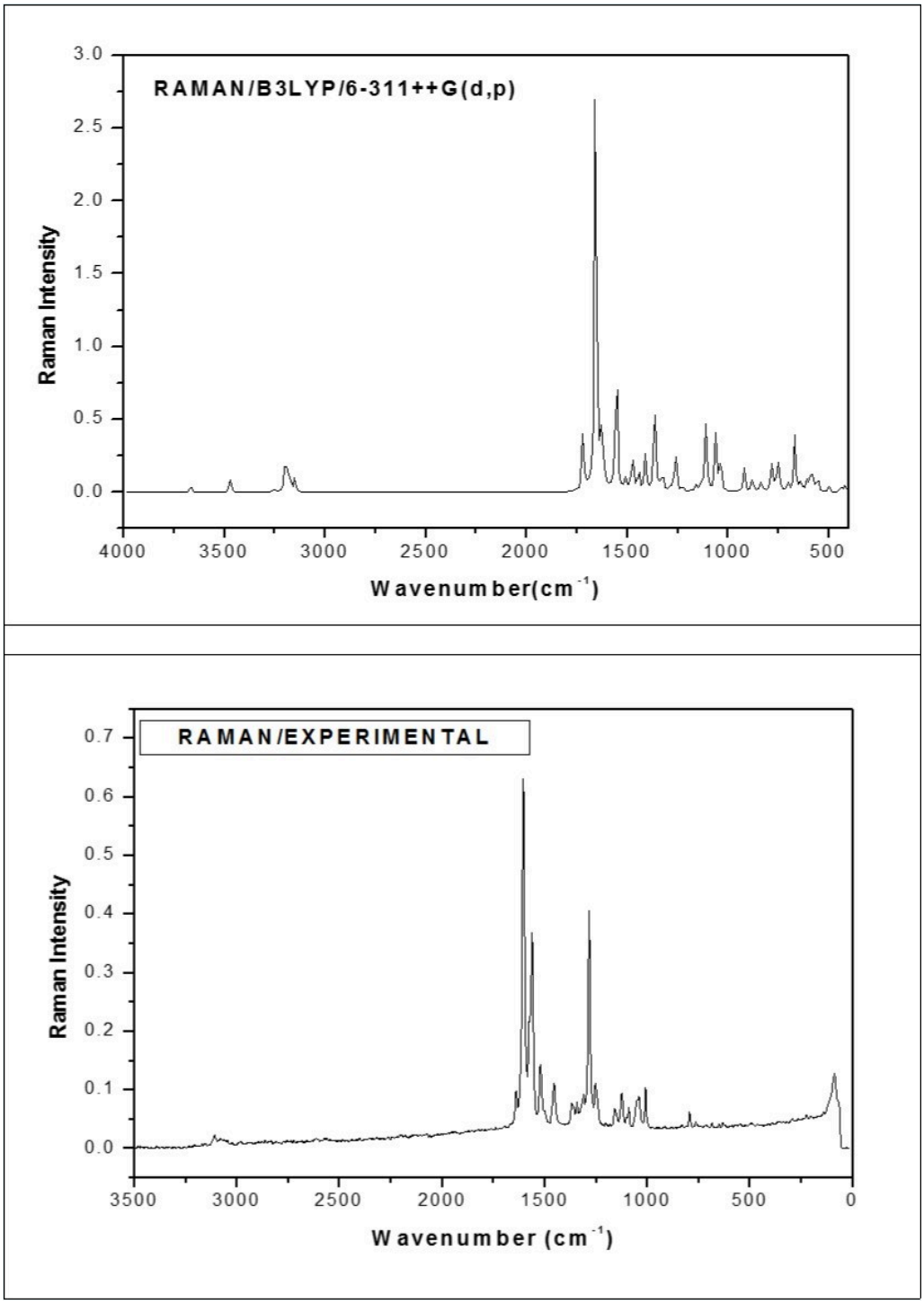


Figure 3. The combined theoretical and experimental FT-Raman spectra of ICINH

OPEN ACCESS

 DOI: 10.14302/issn.2377-2549.jndc-17-1459

Table 2.1 (continued)

S.No	Type	Fragment type	Definition
27,28	C-C	Out-of the ring	C_8-C_{16}, C_{21}-C_{22}
29	C=O		C_{21}-O_{32}
30	N-H		N_{19}-H_{20}
31	C-H		C_{16}-H_{17}
32,33	C-N		C_{16}-N_{18}, C_{21}-N_{19}
34	N-N		N_{18}-N_{19}
In-plane bending			
35-45	C-C(N)-C(N)	Double ring	C_1-C_2 -C_3, C_2-C_3-C_4, C_3-C_4 -C_5, C_4-C_5 -C_6, C_5-C_6 -C_1, C_6-C_1-C_2, C_1-C_2-C_8, C_2-C_8-C_7, C_8-C_7-N_{15}, C_7-N_{15}-C_1
			N_{15}-C_1 -C_2
46-55	C(N)-C-H		C_2-C_3 -H_9, C_4-C_3 -H_9, C_3-C_4 -H_{10}, C_5-C_4 -H_{10}, C_4-C_5 -H_{11}, C_6-C_5 -H_{11}, C_1-C_6 -H_{12}, C_5-C_6 -H_{12}, C_8-C_7 -H_{14}, N_{15}-C_7 -H_{14}
56,57	C-N-H		C_1-N_{15}-H_{13}, C_7-N_{15}-H_{13}
58,59	C-C-C(N)		C_6-C_1-N_{15}, C_3-C_2-C_8
60,61	C-C-H	Out-of the ring	C_8-C_{16}-H_{17}, N_{18}-C_{16}-H_{17}
62,63	C-C-N		C_8-C_{16}-N_{18}, C_{22}-C_{21}-N_{19}
64,65	C-N-N		C_{16}-N_{18}-N_{19}, C_{21}-N_{19}-N_{18}
66,67	C(N)-N-H		C_{21}-N_{19}-H_{20}, N_{18}-N_{19}-H_{20}
68,69	C(N)-C=O		C_{22}-C_{21}-O_{32}, N_{19}-C_{21}-O_{32}
70-73	C-C-C		C_{21}-C_{22} -C_{23}, C_{21}-C_{22}-C_{24}, C_2-C_8 -C_{16}, C_7-C_8-C_{16}
74-79	C-C(N)-C(N)	Pyridine ring	C_{22}-C_{23} -C_{25}, C_{23}-C_{25}-C_{28}, C_{25}-C_{28} -N_{31}, C_{28}-N_{31}-C_{24}, N_{31}-C_{24}-C_{22}, C_{24}-C_{22}-C_{23}
80-87	C(N)-C-H		C_{22}-C_{23}-H_{26}, C_{25}-C_{23}-H_{26}, C_{22}-C_{24}-H_{27}, N_{31}-C_{24}-H_{27}, C_{23}-C_{25}-H_{29}, C_{28}-C_{25}-H_{29}, C_{25}-C_{28}-H_{30}, N_{31}-C_{28}-H_{30}
Out-of-plane bending			
88-98	C(N)-C(N)-C(N)-C(N)	Double ring	C_1-C_2-C_3-C_4, C_2-C_3-C_4-C_5, C_3-C_4-C_5-C_6, C_4-C_5 -C_6-C_1, C_5-C_6-C_1-C_2, C_6-C_1-C_2-C_3, C_1-C_2 -C_8-C_7, C_2-C_8-C_7-N_{15}, C_8-C_7-N_{15}-C_1, C_7-N_{15}-C_1-C_2, N_{15}-C_1 -C_2-C_8
99-103	H-C(N)-C-C(N)		H_9-C_3-C_2-C_4, H_{10}-C_4-C_3-C_5, H_{11}-C_5-C_4-C_6, H_{12}-C_6-C_1-C_5, H_{13}-N_{15}-C_1-C_7, H_{14}-C_7-C_8-N_{15}

Table 2.1 (continued)

S.No	Type	Fragment type	Definition
105,106	C-C-C-C	Out-of the ring	C_{16}-C_8-C_2-C_7, C_{21}-C_{22}-C_{23}-C_{24}
107	O-C-C-N		O_{32}-C_{21}-C_{22}-N_{19}
108	H-N-N-C		H_{20}-N_{19}-N_{18}-C_{21}
109	H-C-C-N		H_{17}-C_{16}-C_8-N_{18}
110	C-N-N-C		C_{16}-N_{18}-N_{19}-C_{21}
111-114	N-C-C-C		N_{19}-C_{21}-C_{22}-C_{23}, N_{19}-C_{21}-C_{22}-C_{24},
			C_2- C_8- C_{16}-N_{18}, C_7-C_8-C_{16}-N_{18}
115-120	C(N)-C(N)-C(N)-C(N)	Pyridine	C_{22}-C_{23}-C_{25}-C_{28}, C_{23}-C_{25}-C_{28}-N_{31}, C_{25}-C_{28}-N_{31}-C_{24}, C_{28}-N_{31}-C_{24}-C_{22}, N_{31}-C_{24}-C_{22}-C_{23}, C_{24}-C_{22}-C_{23}-C_{25}
121-124	H-C-C-C		H_{26}-C_{23}-C_{22}-C_{25}, H_{27}-C_{24}-C_{22}-N_{31}, H_{29}-C_{25}-C_{23}-C_{28}, H_{30}-C_{28}-C_{25}-N_{31}
125,126	C(N)-C-C-C	Torsion	C_3-C_2-C_8-C_{16}, N_{15}-C_7-C_8-C_{16}
127,128	C-C-C-C(N)	Butterfly	C_8-C_2-C_1-C_6, C_3-C_2-C_1-N_{15}

Table 2.2. Local Symmetry coordinates of ICINH

S.No	Type	Fragment type	Definition
1-8	C-C	Double ring	R_1, R_2, R_3, R_4, R_5, R_6, R_7, R_8
9,10	C-N		R_9, R_{10}
11-15	C-H		R_{11}, R_{12}, R_{13}, R_{14}, R_{15}
16	N-H		R_{16}
17-20	C-C	Pyridine ring	R_{17}, R_{18}, R_{19}, R_{20}
21,22	C-N		R_{21}, R_{22}
23-26	C-H		R_{23}, R_{24}, R_{25}, R_{26}
27,28	C-C	Out-of the ring	R_{27}, R_{28}
29	C=O		R_{29}
30	N-H		R_{30}
31	C-H		R_{31}
32,33	C-N		R_{32}, R_{33}
34	N-N		R_{34}

 DOI: 10.14302/issn.2377-2549.jndc-17-1459

Table 2.2 (continued)

S.No	Type	Fragment type	Definition
In-plane bending			
35	C(N)-C(N)-C(N)	Double ring	$(\beta_{35}-\beta_{36}+\beta_{37}-\beta_{38}+\beta_{39}-\beta_{40})/\sqrt{6}$
36			$(-\beta_{35}-\beta_{36}+2\beta_{37}-\beta_{38}+\beta_{39}-2\beta_{40})/\sqrt{12}$
37			$(\beta_{35}-\beta_{36}-\beta_{38}-\beta_{39})/\sqrt{2}$
38			$\beta_{41}+a(\beta_{42}+\beta_{45})+b(\beta_{43}+\beta_{44})$
39			$(a-b)(\beta_{41}-\beta_{44})+(1-a)(\beta_{42}-\beta_{43})$
40-44	C(N)-C-H		$(\beta_{46}-\beta_{47})/\sqrt{2}$, $(\beta_{48}-\beta_{49})/\sqrt{2}$, $(\beta_{50}-\beta_{51})/\sqrt{2}$, $(\beta_{52}-\beta_{53})/\sqrt{2}$, $(\beta_{54}-\beta_{55})/\sqrt{2}$
45	C-N-H		$(\beta_{56}-\beta_{57})/\sqrt{2}$
46,47	C(N)-C(N)-C(N)		β_{58}, β_{59}
48	C-C-H	Out-of the ring	$(\beta_{60}-\beta_{61})/\sqrt{2}$
49,50	C-C-N		β_{62}, β_{63}
51	C-N-N		$(\beta_{64}-\beta_{65})/\sqrt{2}$
52	C(N)-N-H		$(\beta_{66}-\beta_{67})/\sqrt{2}$
53	C(N)-C=O		$(\beta_{68}-\beta_{69})/\sqrt{2}$
54,55	C-C-C		$(\beta_{70}-\beta_{71})/\sqrt{2}$, $(\beta_{72}-\beta_{73})/\sqrt{2}$
56	C-C(N)-C(N)	Pyridine ring	$(\beta_{74}-\beta_{75}+\beta_{76}-\beta_{77}+\beta_{78}-\beta_{79})/\sqrt{6}$
57			$(-\beta_{74}-\beta_{75}+2\beta_{76}-\beta_{77}-\beta_{78}+2\beta_{79})/\sqrt{12}$
58			$(\beta_{74}-\beta_{75}-\beta_{77}-\beta_{78})/2$
59-62	C(N)-C-H		$(\beta_{80}-\beta_{81})/\sqrt{2}$, $(\beta_{82}-\beta_{83})/\sqrt{2}$, $(\beta_{84}-\beta_{85})/\sqrt{2}$, $(\beta_{86}-\beta_{87})/\sqrt{2}$
Out-of-plane bending			
63	C(N)-C(N)-C(N)-C(N)	Double ring	$(\gamma_{88}-\gamma_{89}+\gamma_{90}-\gamma_{91}+\gamma_{92}-\gamma_{93})/\sqrt{6}$
64			$(-\gamma_{88}+2\gamma_{89}-\gamma_{90}-\gamma_{91}+2\gamma_{92}-\gamma_{93})/\sqrt{12}$
65			$(\gamma_{88}-\gamma_{89}+\gamma_{90}-\gamma_{91})/\sqrt{2}$
66			$b(\gamma_{94}+\gamma_{98})+a(\gamma_{95}+\gamma_{97})+\gamma_{96}$
67			$(a-b)(\gamma_{98}-\gamma_{94})+(1-a)(\gamma_{97}-\gamma_{95})$
68-73	H-C(N)-C-C(N)		γ_{99}, γ_{100}, γ_{101}, γ_{102}, γ_{103}, γ_{104}

 DOI: 10.14302/issn.2377-2549.jndc-17-1459

Table 2.2 (continued)

S.No	Type	Fragment type	Definition
74,75	C-C-C-C	Out-of the ring	γ_{105}, γ_{106}
76	O-C-C-N		γ_{107}
77	H-N-N-C		γ_{108}
78	H-C-C-N		γ_{109}
79	C-N-N-C		γ_{110}
80,81	N-C-C-C		$(\gamma_{111}-\gamma_{112})/\sqrt{2}$, $(\gamma_{113}-\gamma_{114})/\sqrt{2}$
82	C(N)-C(N)-C(N)-C(N)	Pyridine	$(\gamma_{115}-\gamma_{116}+\gamma_{117}-\gamma_{118}+\gamma_{119}-\gamma_{120})/\sqrt{6}$
83			$(\gamma_{115}-\gamma_{117}+\gamma_{118}-\gamma_{119})/2$
84			$(-\gamma_{115}+2\gamma_{116}-\gamma_{117}-\gamma_{118}+2\gamma_{119}-\gamma_{120})/\sqrt{12}$
85-88	H-C-C-C		γ_{121}, γ_{122}, γ_{123}, γ_{124}
89	C(N)-C-C-C	Ring Torsion	$(\gamma_{125}-\gamma_{126})/\sqrt{2}$
90	C-C-C-C(N)	Butterfly	$(\gamma_{127}-\gamma_{128})/\sqrt{2}$

Table 2.3. The experimental and calculated frequencies of ICINH using B3LYP/6-311++G(d,p) level of basis set [harmonic frequencies (cm^{-1}), IR, Raman intensities (Km/mol), reduced masses (amu) and force constants ($mdynA^{\circ -1}$)]

Mode No	Exp. IR	Exp. Raman	Frequencies	Scaled frequencies	Red. Masses	Force constants	IR Intensity	Raman Intensity	Vibrational Assignments
1	-	-	23	22	5.6685	0.0017	0.05	41.46	γ_{ring} (90)
2	-	-	31	30	6.2039	0.0035	0.26	47.75	γ_{ring} (93)
3	-	-	38	37	4.7887	0.0041	0.29	50.62	γ(py)ring (97)
4	-	-	73	70	6.1906	0.0192	0.52	0.88	γ(py)ring (98)
5	-	89	93	90	6.2748	0.0318	0.06	10.04	γ_{ring} (89)
6	-	-	132	128	6.7417	0.0692	0.31	3.54	$\gamma_{C=O}$ (69), γ_{ring} (23)
7	-	-	151	146	5.367	0.0716	0.35	3.71	γ_{ring} (66), γ_{N-N} (26)
8	-	-	171	166	4.8316	0.0835	0.20	5.00	γ_{N-N}(54), γ_{ring} (37)
9	-	-	196	190	5.1729	0.1176	0.19	3.45	γ(py)ring (67), Butterfly (21)
10	-	-	223	216	4.1358	0.1213	2.07	1.51	Butterfly (89)
11	-	-	236	229	5.5815	0.1835	2.48	4.94	$\beta_{(py)}$ring (78)
12	-	-	295	285	7.0353	0.3595	0.36	0.27	τ_{ring} (94)
13		-	376	363	5.8348	0.4847	0.80	0.48	γ_{ring} (62), γ_{outC-C}(21)

 DOI: 10.14302/issn.2377-2549.jndc-17-1459

Table 2.3 (continued)

Mode No	Exp. IR	Exp. Raman	Frequencies	Scaled frequencies	Red. Masses	Force constants	IR Intensity	Raman Intensity	Vibrational Assignments
14	-	-	402	389	3.5462	0.3379	0.58	1.55	γ_{outC-N}(43), γ_{N-N}(18), γ_{ring}(14)
15	-	-	418	405	5.2085	0.5367	0.63	1.35	γ_{ring} (69), γ(py) ring (24)
16	-	-	426	412	2.5799	0.2753	6.89	0.44	γ_{outC-C}(50), β_{C-N}(22), β_{N-H}(10)
17	426	-	440	426	1.5194	0.1731	7.82	0.87	γ_{N-H}(78)
18	-	-	449	434	3.4966	0.415	3.38	0.38	γ_{outC-C}(56), γ_{C-H} (22)
19	-	-	498	482	5.8526	0.8561	0.62	1.60	β_{ring} (49), γ_{out}C−C(19), γ_{ring} (18)
20	-	-	552	535	5.1322	0.9221	1.85	2.76	$\gamma_{C=N}$(61), γ_{ring} (26)
21	-	-	563	545	5.496	1.0281	0.54	2.03	β_{ring} (72)
22	-	-	582	564	2.8828	0.5762	1.76	4.01	β_{out}C-C (46), β_{N-H} (23)
23	-	-	589	570	3.2755	0.6698	7.32	2.24	γ_{out}N−H(63), β_{C-H} (18)
24	581	-	606	587	5.2868	1.1458	11.97	3.94	$\beta_{(py)}$ring (68), γ_{out}N−H(22)
25	615	-	637	616	6.325	1.5108	2.52	1.88	β_{out}C-C (58), β_{C-H} (20), β_{N-H} (14)
26	-	-	643	623	2.7471	0.6694	0.95	1.01	β_{ring} (52), γ_{C-H} (24)
27	-	-	668	647	2.6474	0.6964	2.08	15.49	β_{N-N} (50), β_{C-N} (18), $\beta_{(py)}$ring (14)
28	682	-	702	679	4.4972	1.3055	1.36	2.28	β_{ring} (51), $\beta_{(py)}$ring (27)
29	-	-	719	696	2.1818	0.6637	3.21	0.31	β_{out}C-C (47), β_{out}C−H (20), β_{ring} (17)
30	-	-	748	724	3.0533	1.0053	12.23	4.31	β_{out}C-N (57), β_{py}ring (18), $\beta_{C=O}$ (13)
31	-	-	751	727	1.4353	0.477	18.39	0.67	γ_{C-H} (79)
32	-	-	754	730	4.3578	1.4603	3.85	4.77	γ_{C-H} (74), $\beta_{(py)}$ring (13)
33	752	-	774	749	3.9285	1.3867	0.53	1.49	β_{out}C-H (48), β_{ring} (21)

 DOI: 10.14302/issn.2377-2549.jndc-17-1459

Table 2.3 (continued)

Mode No	Exp. IR	Exp. Raman	Frequencies	Scaled frequencies	Red. Masses	Force constants	IR Intensity	Raman Intensity	Vibrational Assignments
34	-	-	784	759	4.6888	1.6972	4.98	9.52	β_{ring} (56), $\beta_{(py)}$ring (23)
35	793	795	828	802	1.3744	0.5555	1.89	1.51	γ_{C-H} (88)
36	-	-	840	813	1.9452	0.808	2.26	1.91	γ(py)C-H (92)
37	830	-	855	828	1.4952	0.6446	0.98	0.25	$\beta_{C=O}$ (60), $\beta_{(py)}$ring (19)
38	-	-	877	849	3.9613	1.796	23.55	3.59	$\beta_{C=N}$ (45), β_{ring} (24), $\beta_{(py)}$ring (18)
39	-	-	893	864	4.4426	2.0861	3.75	0.23	β_{ring} (78)
40	-	-	919	890	1.4668	0.7301	1.25	6.07	γ_{C-H} (91)
41	912	-	944	913	1.3666	0.717	0.23	0.11	γ_{C-H} (87)
42	-	-	949	919	1.3956	0.7404	0.86	0.11	γ(py)C-H (90)
43	-	-	981	949	1.2808	0.7258	0.01	0.06	β_{N-H} (59), β_{C-H}(21)
44	953	-	986	955	1.4487	0.8303	0.17	0.01	γ(py)C-H (92)
45	-	-	1006	974	1.3774	0.8218	0.47	0.09	γ(py)C-H (92)
46	-	-	1035	1002	2.1293	1.3435	1.87	6.90	υ_{C-C} (41), β_{C-H} (28)
47	1006	1009	1040	1007	4.2574	2.715	2.20	2.57	$\upsilon_{(py)}$C-C (52), $\beta_{(py)}$C–H (29)
48	-	-	1059	1025	3.2592	2.1539	0.09	13.50	$\upsilon_{(py)}$C-C (68), $\beta_{(py)}$C–H (24)
49	1047	1041	1066	1032	4.5472	3.0425	4.45	1.84	υ_{out}C-C (45), β_{ring} (20), β_{C-H} (14)
50	-	-	1109	1074	3.4326	2.4881	18.31	16.64	υ_{N-N}(52), $\beta_{(py)}$C–H (18), β_{out}C–H (13)
51	-	1092	1129	1093	1.5981	1.2012	5.03	1.73	β C-H (47), β_{N-H} (22), υ_{C-N}(17)
52	-	-	1139	1102	1.4616	1.1167	0.86	0.43	$\beta_{(py)}$C-H (50), $\upsilon_{(py)}$C–C (27)
53	-	-	1155	1118	1.4763	1.1596	8.68	0.69	β_{C-H} (69)
54	1126	1125	1160	1123	2.4869	1.9719	14.10	1.24	υ_{out}C-C (42), υ_{out}C–N (28) $\beta_{(py)}$C–H (15),
55	-	-	1178	1140	1.1543	0.9431	0.36	0.39	υ_{C-C} (53), υ_{C-N} (19), β_{C-H} (15)

 DOI: 10.14302/issn.2377-2549.jndc-17-1459

Table 2.3 (continued)

Mode No	Exp. IR	Exp. Raman	Frequencies	Scaled frequencies	Red. Masses	Force constants	IR Intensity	Raman Intensity	Vibrational Assignments
56	-	-	1225	1186	1.4787	1.3081	2.73	1.51	$\beta_{(py)}$C-H (72), $\upsilon_{(py)}$C–N (20)
57	-	-	1251	1211	2.7583	2.5422	12.80	0.79	β_{C-H} (52), υ_{C-N}(18), β_{N-H} (14)
58	-	-	1263	1222	1.8362	1.7252	7.35	10.89	υ_{C-N} (54), β_{C-H} (31)
59	1244	1254	1285	1244	7.2124	7.0219	2.07	1.25	$\upsilon_{(py)}$C-N (59), $\beta_{(py)}$C–H (22)
60	-	1284	1325	1282	2.4286	2.5111	0.37	5.82	υ_{C-C} (62), β_{C-H} (20)
61	1298	-	1339	1296	2.3836	2.5178	54.46	0.89	β C–H (49), υ_{C-N}(19), β_{out}C–H (17)
62	-	-	1361	1318	3.0228	3.3	71.69	18.10	$\upsilon_{(py)}$ C–C (50), β_{C-H} (21), υ_{out}C–C (12)
63	-	-	1365	1322	1.2876	1.4144	0.50	0.80	υ_{out}C–N (58), β_{C-H} (23)
64	1336	1345	1371	1327	5.9533	6.5908	6.32	4.61	υ_{C-C} (72), β_{C-H} (21)
65	1360	1368	1410	1364	1.5509	1.8154	16.15	8.86	β_{out}C–H (59), υ_{C-N} (15), β_{N-H} (12)
66	-	-	1442	1396	2.1721	2.6626	6.54	4.66	υ_{C-C} (49), β_{C-H} (27)
67	1408	-	1447	1401	2.2447	2.7699	2.37	1.22	$\beta_{(py)}$C–H (65), $\upsilon_{(py)}$ (24)
68	-	-	1473	1426	1.7655	2.2568	30.11	9.65	β_{out}N-H (60), υ_{out}C-N (17), υ_{out}C–C (14)
69	-	-	1483	1436	2.3645	3.064	4.89	0.81	β_{C-H} (54), υ_{C-C} (21), β_{out}N–H (18)
70	1447	1455	1508	1460	2.2353	2.9957	1.61	3.14	$\beta_{(py)}$ C-H (48), $\upsilon_{(py)}$ (23), υ_{out}C-C (10)
71	-	-	1524	1475	2.7967	3.8252	0.94	0.21	υ_{C-N} (43), υ_{C-C} (24), β_{C-H} (18)
72	1501	-	1554	1505	4.4312	6.307	20.77	41.94	$\upsilon_{C=C}$ (68), β_{C-H} (19)
73	-	-	1604	1553	5.2119	7.9032	1.13	0.34	$\upsilon_{(py)}$ C–C (69), β_{C-H} (22)
74	-	1563	1615	1563	5.7905	8.8973	0.09	6.24	υ_{C-C} (53), β_{N-H} (25)

Table 2.3 (continued)

Mode No	Exp. IR	Exp. Raman	Frequencies	Scaled frequencies	Red. Masses	Force constants	IR Intensity	Raman Intensity	Vibrational Assignments
75	-	-	1628	1575	5.6711	8.851	11.33	13.99	$\upsilon_{(py)}$ C–N (56), $\upsilon_{(py)}$C–C (23), $\beta_{(py)}$C–H(14)
76	-	-	1657	1604	7.6432	12.3614	5.91	100.00	$\upsilon_{out.}$C=N (56), υ_{C-C} (23), β_{C-H} (14)
77	1608	1606	1658	1605	6.6961	10.8407	2.95	28.60	υ_{C-C} (52), $\upsilon_{C=N}$ (28), β_{C-H} (12)
78	1677	-	1718	1663	7.9762	13.8766	100.00	14.72	$\upsilon_{C=O}$ (71), β_{N-H} (23)
79	-	-	3147	3046	1.0879	6.3482	1.02	0.82	$\upsilon_{out.}$C–H (98)
80	-	-	3150	3049	1.0892	6.366	4.06	2.60	$\upsilon_{as(py)}$ C–H (95)
81	-	-	3167	3066	1.0858	6.4172	0.15	0.55	υ_{as}C–H (96)
82	3078	-	3174	3073	1.0887	6.463	0.72	2.26	υ_{as}C–H (96)
83	-	-	3184	3082	1.0936	6.532	4.39	1.24	υ_{as}C–H (95)
84	-	-	3185	3083	1.0909	6.5186	2.94	2.80	$\upsilon_{as(py)}$C–H (92)
85	-	-	3194	3092	1.0971	6.5933	3.03	5.67	υ_{s}C–H (97)
86	-	-	3201	3099	1.092	6.593	2.66	0.24	$\upsilon_{as(py)}$C–H (91)
87	3107	3109	3202	3100	1.0948	6.6134	0.13	3.81	$\upsilon_{as(py)}$C–H (94)
88	3159	-	3253	3149	1.097	6.8395	0.27	0.60	υ_{C-H} (99)
89	-	-	3471	3360	1.0748	7.6289	7.50	3.16	$\upsilon_{out.}$N–H (99)
90	3531	-	3664	3540	1.0805	8.5473	21.55	1.77	υ_{N-H} (100)

υ: Stretching, β: in-plane-bending, Γ: out-of-plane bending, τ: Torsion, vw: very week, w: week, m: medium, s: strong, vs: very strong,
[a] Scaling factor: 0.9608 (Radom et al., 1970 and Pople et al., 1993),
[b] Relative IR absorption intensities normalized with highest peak absorption equal to 100,
[c] Relative Raman intensities calculated by Equation (2.1) and normalized to 100,
[d] Total energy distribution calculated at B3LYP/6-311++G(d,p) level.

Ring Vibrations

The ring stretching vibrations are very prominent in the spectrum of pyridine and its derivatives and are highly characteristic of aromatic ring itself [18]. The C–C stretching vibrations of pyridine derivatives usually appear in the region between 1650–1400 cm^{-1} and 1100–1000 cm^{-1} [19]. In the present study, the peaks identified at 1006 cm^{-1} in FT-IR and 1009 cm^{-1} in FT-Raman are assigned to C–C stretching vibrations. Due to the absence of peaks, the theoretically scaled values at 1553, 1318 and 1025 cm^{-1} are assigned as C–C stretching vibrations of the rest of other modes in pyridine ring. The presence of nitrogen in the ring of the pyridine structure gives rise to two C–N stretching vibrations. Identifying these vibrations is rather a difficult task as their vibrational frequency lies within the C–C stretching region. As expected, the peaks for C–N stretching vibrations are found at 1244 cm^{-1} in FT-IR and 1254 cm^{-1} in FT-Raman spectrum. The theoretically scaled values of this mode are found to be in good agreement with experimental values.

 DOI: 10.14302/issn.2377-2549.jndc-17-1459

According to PED results, the C−C stretching vibrations of six and five members are assigned. The C−C stretching vibrations are observed at 1608, 1501 and 1336 cm^{-1} in FT-IR and 1606, 1563, 1345 and 1284 cm^{-1} in FT-Raman spectrum. The theoretically predicted scaled values are in excellent correlation with that of the experimental values.

C−H Vibrations

Four C−H bonds in the pyridine ring of the title molecule give rise to four C−H stretching vibrations. The hetero-aromatic structure shows the presence of C−H stretching vibrations in the region 3000−3100 cm^{-1} [20], which is the characteristic region for ready identification of this structure. In this region, the bands are not affected appreciably by the nature of the substituents. In the present study, the peak at 3107 cm^{-1} in FT-IR and at 3109 cm^{-1} in FT-Raman are assigned to C−H stretching vibrations of the pyridine ring. The percentage of PED results show that these modes are very pure modes. Similarly, the peaks appearing at 3159 and 3078 cm^{-1} in FT-IR are ascribed to C−H stretching vibrations of the benzene ring of the title molecule.

C=O Vibrations

The characteristic IR absorption wavenumber of C=O is normally strong in intensity and found in the region 1600–1800 cm^{-1} [21], [22]. In the present study, the strong peak at 1677 cm^{-1} in FT-IR is assigned to C=O stretching. The calculated value of C=O stretching mode at B3LYP/6-311++G(d,p) shows good agreement with the experimental value. The C=O in-plane bending vibration is identified at 830 cm^{-1} in FT-IR. A peak for C=O out-of-plane bending vibration is not active in both IR and Raman spectra. Hence the theoretically predicted value (128 cm^{-1}/mode no: 6) is assigned to this mode.

N−H Vibrations

In primary amines, usually the N–H stretching vibrations occur in the region 3600–3300 cm^{-1} [23]. In the present study, the N–H bond in the five-membered ring produces a well defined peak at 3531 cm^{-1} in FT-IR. A peak for the N_{19}–H_{20} bond present at the out-of-the ring is not active in both IR and Raman. Hence, the theoretical scaled value of 3540 cm^{-1} is assigned to N_{15}–H_{13} stretching mode. All the vibrations in this group are in excellent agreement with experimental results as well as with literature [24].

C=N and N−N Vibrations

The identification of C=N stretching vibrations is a difficult task since these are usually coupled with ring stretching and C-H in-plane bending vibrations. A bond C_{21}=N_{19} at out of the ring possesses three vibrational normal modes. Since all these vibrations are inactive in both the spectra, the theoretically predicted wavenumbers 1604, 849 and 535 cm^{-1} are ascribed to C=N stretching, in-plane bending and out-of-plane bending, respectively. Similarly, the N−N stretching and bending vibrations are not present in both IR and Raman. Hence, the theoretically scaled values of 1074, 647 and 166 cm^{-1} are attributed to N−N stretching, in-plane bending and out-of-plane bending vibrations, respectively.

NLO Property

Non linear effect arise from the interactions of electromagnetic fields in various media to produce new fields altered in phase, frequency, amplitude or other propagation characteristics from incident fields [25]. The first hyperpolarizability (β_0), dipole moment μ and polarizability α are calculated using DFT/6-311++G(d,p) basis set. The computed total static dipole moment (μ), the mean polarizability (α_0), the mean first hyperpolarizability (β_0), for the molecule under study are presented in Table 3 shows that the first order hyperpolarizability value plays an important role in determining the NLO activity of the molecule. The first order hyperpolarizability (β_0) of the present molecule is $8.6424x10^{-30}$ esu while that of urea is $0.3728x10^{-30}$ esu. The (β_o) of ICINH is 23 times greater than that of urea, hence, the molecule can be said to have high NLO activity; which is naturally due to the contribution of oxygen atom which makes one part of molecule highly negative and other part as equally positive.

Table 3. The NLO measurements of ICINH

Parameters	B3LYP/6-311++G(d,p)
Dipole moment (μ) Debye	
μ_x	1.6403
μ_y	0.4934
μ_z	0.1242
M	1.7174Debye
Polarizability (α_0) x10^{-30}esu	
α_{xx}	351.00
α_{xy}	-4.96
α_{yy}	194.94
α_{xz}	1.53
α_{yz}	4.90
α_{zz}	132.91
α_o	0.5902x10^{-30}esu
Hyperpolarizability (β_0) x10^{-30}esu	
β_{xxx}	-1163.89
β_{xxy}	31.69
β_{xyy}	148.04
β_{yyy}	-106.30
β_{xxz}	-196.67
β_{xyz}	-19.08
β_{yyz}	12.83
β_{xzz}	46.85
β_{yzz}	-42.47
β_{zzz}	-35.40
β_0	8.6424x10^{-30}esu

Standard value for urea (μ=1.3732 Debye, β_0=0.3728x10^{-30}esu): esu-electrostatic unit

NBO Analysis

The NBO analysis is performed on ICINH using B3LYP/6-311++G(d,p) basis set and are listed in Table 4. In the study, the π bonds have higher ED than the σ bonds. Due to this reason, the σ-σ* transitions have minimum delocalization energy than the π-π* transitions. It is evident from the Table 4. The ED of π(C_{30}-N_{32}) bond transfer energy 116.4, 52.38 kJ/mol to the acceptor orbitals: C_{22}-C_{24} and C_{23}-C_{25}, respectively. There occurs a strong intra-molecular hyperconjugative interaction of π electron

from C_{23}-C_{25} bond to the π*C_{22}-C_{24}→C_{30}-N_{32} bonds, which increases the EDs: 0.3281 and 0.3727 kJ/mol, respectively. The lone pair electrons are readily available for the interaction with excited electrons of antibonding orbital. During n-π* transition, more energy delocalization takes place: N_{19}→C_{16}-N_{18}; C_{21}→O_{29} and N_{15}→C_1-C_2; C_7-C_8. The corresponding excitation energy values are 102.42, 170.41 and 140.71, 160.41, respectively. In which, these (N_{19}→C_{21}-O_{29} & N_{15}→C_7-C_8) two transitions give the strongest stabilization to the system.

Table 4. The Second order perturbation theory analysis of Fock Matrix in NBO basis for ICINH

Type	Donor NBO (i)	ED/e	Acceptor NBO (j)	ED/e	[a]E(2)	[b]E(j)-E(i)	[c]F(i,j)
					KJ/mol	a.u.	a.u.
σ -σ*	BD (1) C 1 - C 2	1.959	BD*(1) C 1 - C 6	0.021	18.95	1.23	0.07
			BD*(1) C 2 - C 3	0.022	14.06	1.24	0.06
			BD*(1) C 2 - C 8	0.027	8.20	1.16	0.04
			BD*(1) C 3 - H 9	0.014	10.59	1.11	0.05
			BD*(1) C 6 - H 12	0.013	9.41	1.10	0.05
			BD*(1) C 8 - C 16	0.036	17.95	1.15	0.06
			BD*(1) H 13 - N 15	0.016	16.82	1.04	0.06
π -π*	BD (2) C 1 - C 2	1.596	BD*(2) C 3 - C 4	0.301	79.16	0.29	0.07
			BD*(2) C 5 - C 6	0.319	76.11	0.28	0.07
			BD*(2) C 7 - C 8	0.349	78.70	0.26	0.06
σ -σ*	BD (1) C 1 - C 6	1.976	BD*(1) C 1 - C 2	0.027	20.21	1.25	0.07
			BD*(1) C 1 - N 15	0.027	8.91	1.15	0.04
			BD*(1) C 2 - C 8	0.027	5.86	1.21	0.04
			BD*(1) C 5 - C 6	0.013	11.59	1.30	0.05
			BD*(1) C 5 - H 11	0.012	9.46	1.16	0.05
			BD*(1) C 6 - H 12	0.014	4.18	1.14	0.03
			BD*(1) C 7 - N 15	0.013	6.53	1.15	0.04
σ -σ*	BD (1) C 1 - N 15	1.986	BD*(1) C 1 - C 2	0.027	4.44	1.36	0.03
			BD*(1) C 1 - C 6	0.021	8.54	1.38	0.05
			BD*(1) C 2 - C 3	0.022	9.87	1.38	0.05
			BD*(1) C 7 - H 14	0.012	9.12	1.23	0.05
			BD*(1) C 7 - N 15	0.013	6.40	1.26	0.04
σ -σ*	BD (1) C 2 - C 3	1.974	BD*(1) C 1 - C 2	0.027	15.44	1.24	0.06
			BD*(1) C 1 - N 15	0.027	7.11	1.13	0.04
			BD*(1) C 2 - C 8	0.027	18.79	1.19	0.07

 DOI: 10.14302/issn.2377-2549.jndc-17-1459

Table 4 (continued)

Type	Donor NBO (i)	ED/e	Acceptor NBO (j)	ED/e	[a]E(2)	[b]E(j)-E(i)	[c]F(i,j)
					KJ/mol	a.u.	a.u.
			BD*(1) C 3 - C 4	0.014	12.47	1.29	0.06
			BD*(1) C 4 - H 10	0.013	9.33	1.15	0.05
σ -σ*	BD (1) C 2 - C 8	1.962	BD*(1) C 1 - C 2	0.027	8.37	1.20	0.04
			BD*(1) C 1 - C 6	0.021	15.82	1.22	0.06
			BD*(1) C 1 - N 15	0.026	4.18	1.09	0.03
			BD*(1) C 2 - C 3	0.022	16.48	1.22	0.06
			BD*(1) C 3 - C 4	0.013	5.10	1.25	0.04
			BD*(1) C 7 - C 8	0.019	12.84	1.21	0.06
			BD*(1) C 7 - H 14	0.012	18.95	1.07	0.06
			BD*(1) C 7 - N 15	0.013	5.44	1.09	0.03
			BD*(1) C 8 - C 16	0.036	10.08	1.13	0.05
			BD*(1) C 16 - N 18	0.010	9.50	1.25	0.05
σ -σ*	BD (1) C 3 - C 4	1.978	BD*(1) C 2 - C 3	0.023	13.77	1.27	0.06
			BD*(1) C 2 - C 8	0.027	19.25	1.19	0.07
			BD*(1) C 3 - H 9	0.014	4.69	1.14	0.03
			BD*(1) C 4 - C 5	0.016	10.84	1.26	0.05
			BD*(1) C 5 - H 11	0.012	8.49	1.15	0.04
π -π*	BD (2) C 3 - C 4	1.721	BD*(2) C 1 - C 2	0.477	75.10	0.28	0.07
			BD*(2) C 5 - C 6	0.319	82.34	0.28	0.07
σ -σ*	BD (1) C 3 - H 9	1.979	BD*(1) C 1 - C 2	0.027	17.24	1.06	0.06
			BD*(1) C 4 - C 5	0.016	16.07	1.08	0.06
σ -σ*	BD (1) C 4 - C 5	1.979	BD*(1) C 3 - C 4	0.013	11.17	1.28	0.05
			BD*(1) C 3 - H 9	0.014	10.46	1.13	0.05
			BD*(1) C 5 - C 6	0.013	10.92	1.27	0.05
			BD*(1) C 6 - H 12	0.013	11.05	1.12	0.05
σ -σ*	BD (1) C 4 - H 10	1.980	BD*(1) C 2 - C 3	0.022	15.98	1.08	0.06
			BD*(1) C 5 - C 6	0.013	15.94	1.10	0.06
σ -σ*	BD (1) C 5 - C 6	1.976	BD*(1) C 1 - C 6	0.021	13.97	1.27	0.06
			BD*(1) C 1 - N 15	0.026	25.98	1.14	0.08
			BD*(1) C 4 - C 5	0.015	10.54	1.27	0.05

 DOI: 10.14302/issn.2377-2549.jndc-17-1459

Table 4 (continued)

Type	Donor NBO (i)	ED/e	Acceptor NBO (j)	ED/e	[a]E(2)	[b]E(j)-E(i)	[c]F(i,j)
					KJ/mol	a.u.	a.u.
			BD*(1) C 4 - H 10	0.012	8.28	1.15	0.04
			BD*(1) C 6 - H 12	0.013	5.27	1.13	0.03
π -π*	BD (2) C 5 - C 6	1.729	BD*(2) C 1 - C 2	0.477	82.01	0.28	0.07
			BD*(2) C 3 - C 4	0.301	72.63	0.29	0.06
σ -σ*	BD (1) C 5 - H 11	1.980	BD*(1) C 1 - C 6	0.022	14.69	1.08	0.06
			BD*(1) C 3 - C 4	0.0140	15.69	1.11	0.06
σ -σ*	BD (1) C 6 - H 12	1.980	BD*(1) C 1 - C 2	0.027	17.66	1.07	0.06
			BD*(1) C 4 - C 5	0.016	15.06	1.09	0.06
σ -σ*	BD (1) C 7 - C 8	1.972	BD*(1) C 2 - C 3	0.023	20.42	1.28	0.07
			BD*(1) C 2 - C 8	0.027	12.18	1.21	0.05
			BD*(1) C 7 - H 14	0.012	6.53	1.13	0.04
			BD*(1) C 8 - C 16	0.036	12.34	1.20	0.05
			BD*(1) H 13 - N 15	0.017	14.02	1.09	0.05
			BD*(1) C 16 - H 17	0.022	4.23	1.13	0.03
π -π*	BD (2) C 7 - C 8	1.801	BD*(2) C 1 - C 2	0.477	66.23	0.30	0.07
			BD*(2) C 7 - C 8	0.349	8.87	0.29	0.02
			BD*(2) C 16 - N 18	0.212	73.60	0.29	0.06
σ -σ*	BD (1) C 7 - H 14	1.984	BD*(1) C 1 - N 15	0.026	12.26	1.01	0.05
			BD*(1) C 2 - C 8	0.027	8.66	1.06	0.04
			BD*(1) C 7 - C 8	0.019	6.07	1.13	0.04
σ -σ*	BD (1) C 7 - N 15	1.985	BD*(1) C 1 - C 6	0.021	17.03	1.39	0.07
			BD*(1) C 1 - N 15	0.026	7.32	1.26	0.04
			BD*(1) C 7 - C 8	0.019	5.06	1.38	0.04
			BD*(1) C 8 - C 16	0.036	16.07	1.30	0.06
σ -σ*	BD (1) C 8 - C 16	1.979	BD*(1) C 1 - C 2	0.027	4.81	1.23	0.03
			BD*(1) C 2 - C 8	0.027	14.31	1.18	0.06
			BD*(1) C 7 - C 8	0.019	14.81	1.24	0.06
			BD*(1) C 7 - N 15	0.013	4.48	1.13	0.03
			BD*(1) C 16 - N 18	0.010	9.54	1.29	0.05
σ -σ*	BD (1) H 13 - N 15	1.990	BD*(1) C 1 - C 2	0.027	7.41	1.24	0.04

 DOI: 10.14302/issn.2377-2549.jndc-17-1459

Table 4 (continued)

Type	Donor NBO (i)	ED/e	Acceptor NBO (j)	ED/e	[a]E(2)	[b]E(j)-E(i)	[c]F(i,j)
					KJ/mol	a.u.	a.u.
			BD*(1) C 7 - C 8	0.019	5.73	1.26	0.04
σ -σ*	BD (1) C 16 - H 17	1.969	BD*(1) C 7 - C 8	0.019	20.08	1.07	0.06
			BD*(1) N 18 - N 19	0.030	35.31	0.89	0.08
σ -σ*	BD (1) C 16 - N 18	1.988	BD*(1) C 2 - C 8	0.027	4.98	1.39	0.04
			BD*(1) C 8 - C 16	0.036	9.37	1.38	0.05
			BD*(1) N 19 - C 21	0.073	10.33	1.33	0.05
π -π*	BD (2) C 16 - N 18	1.942	BD*(2) C 7 - C 8	0.349	32.55	0.35	0.05
σ -σ*	BD (1) N 18 - N 19	1.986	BD*(1) C 16 - H 17	0.022	8.62	1.27	0.05
			BD*(1) C 21 - O 29	0.021	5.69	1.44	0.04
σ -σ*	BD (1) N 19 - H 20	1.983	BD*(1) C 21 - C 22	0.066	15.10	1.09	0.06
σ -σ*	BD (1) N 19 - C 21	1.990	BD*(1) C 16 - N 18	0.010	8.91	1.42	0.05
			BD*(1) C 22 - C 23	0.021	4.39	1.39	0.03
			BD*(1) C 25 - C 23	0.026	4.23	4.67	0.06
σ -σ*	BD (1) C 21 - C 22	1.974	BD*(1) N 19 - H 20	0.042	10.96	1.03	0.05
			BD*(1) C 21 - O 29	0.021	5.27	1.24	0.04
			BD*(1) C 22 - C 23	0.021	7.07	1.23	0.04
			BD*(1) C 22 - C 24	0.033	8.12	1.22	0.04
			BD*(1) C 23 - C 25	0.015	9.08	1.25	0.05
			BD*(1) C 25 - N 32	0.015	9.50	1.21	0.05
σ -σ*	BD (1) C 21 - O 29	1.992	BD*(1) N 18 - N 19	0.030	7.28	1.39	0.04
			BD*(1) C 21 - C 22	0.066	7.11	1.45	0.05
			BD*(1) C 22 - C 24	0.033	5.61	1.59	0.04
π -π*	BD (2) C 21 - O 29	1.979	BD*(2) C 22 - C 24	0.328	13.85	0.42	0.04
σ -σ*	BD (1) C 22 - C 23	1.973	BD*(1) N 19 - C 21	0.073	8.49	1.13	0.04
			BD*(1) C 21 - C 22	0.066	7.07	1.12	0.04
			BD*(1) C 22 - C 24	0.033	14.85	1.26	0.06
			BD*(1) C 23 - C 25	0.0148	10.84	1.29	0.05
			BD*(1) C 24 - H 27	0.023	9.50	1.15	0.05
			BD*(1) C 25 - H 28	0.013	10.59	1.14	0.05
σ -σ*	BD (1) C 22 - C 24	1.979	BD*(1) C 21 - C 22	0.066	6.23	1.13	0.04

 DOI: 10.14302/issn.2377-2549.jndc-17-1459

Table 4 (continued)

Type	Donor NBO (i)	ED/e	Acceptor NBO (j)	ED/e	[a]E(2)	[b]E(j)-E(i)	[c]F(i,j)
					KJ/mol	a.u.	a.u.
			BD*(1) C 21 - O 29	0.021	6.65	1.29	0.04
			BD*(1) C 22 - C 23	0.021	16.07	1.27	0.06
			BD*(1) C 23 - H 26	0.014	10.42	1.16	0.05
			BD*(1) C 24 - H 27	0.023	4.35	1.15	0.03
			BD*(1) C 24 - C 30	0.015	5.90	1.26	0.04
π -π*	BD (2) C 22 - C 24	1.610	BD*(2) C 21 - O 29	0.274	74.39	0.29	0.07
			BD*(2) C 23 - C 25	0.287	97.53	0.28	0.07
			BD*(2) C 28 - N 31	0.372	68.03	0.27	0.06
σ -σ*	BD (1) C 23 - C 25	1.979	BD*(1) C 21 - C 22	0.066	12.01	1.13	0.05
			BD*(1) C 22 - C 23	0.021	12.22	1.27	0.05
			BD*(1) C 25 - H 28	0.014	4.35	1.15	0.03
			BD*(1) C 30 - H 31	0.024	9.25	1.14	0.05
π -π*	BD (2) C 23 - C 25	1.639	BD*(2) C 22 - C 24	0.329	69.33	0.29	0.06
			BD*(2) C 30 - N 32	0.373	123.22	0.27	0.08
σ -σ*	BD (1) C 23 - H 26	1.979	BD*(1) C 22 - C 24	0.033	16.99	1.08	0.06
σ -σ*	BD (1) C 24 - H 27	1.979	BD*(1) C 22 - C 23	0.021	17.45	1.08	0.06
			BD*(1) C 30 - N 32	0.016	20.33	1.06	0.06
σ -σ*	BD (1) C 24 - N 31	1.986	BD*(1) C 21 - C 22	0.066	9.41	1.25	0.05
			BD*(1) C 22 - C 24	0.033	8.12	1.38	0.05
			BD*(1) C 28 - H 30	0.024	8.74	1.25	0.05
σ -σ*	BD (1) C 25 - C 23	1.985	BD*(1) C 23 - C 25	0.015	10.59	1.30	0.05
			BD*(1) C 23 - H 26	0.014	11.63	1.16	0.05
			BD*(1) C 30 - N 32	0.016	5.86	1.26	0.04
σ -σ*	BD (1) C 25 - H 23	1.979	BD*(1) C 22 - C 23	0.021	14.52	1.09	0.06
			BD*(1) C 30 - N 32	0.016	17.87	1.07	0.06
σ -σ*	BD (1) C 30 - H 31	1.982	BD*(1) C 23 - C 25	0.015	14.73	1.11	0.06
			BD*(1) C 25 - N 32	0.015	20.17	1.07	0.06
σ -σ*	BD (1) C 30 - N 32	1.987	BD*(1) C 24 - H 27	0.023	8.79	1.27	0.05
			BD*(1) C 25 - H 29	0.013	6.11	1.26	0.04
π -π*	BD (2) C 30 - N 32	1.705	BD*(2) C 22 - C 24	0.328	116.40	0.32	0.09

Table 4 (continued)

Type	Donor NBO (i)	ED/e	Acceptor NBO (j)	ED/e	[a]E(2)	[b]E(j)-E(i)	[c]F(i,j)
					KJ/mol	a.u.	a.u.
			BD*(2) C 23 - C 25	0.287	52.38	0.32	0.06
n -π*	LP (1) N 15	1.613	BD*(2) C 1 - C 2	0.476	140.71	0.30	0.09
			BD*(2) C 7 - C 8	0.349	160.41	0.29	0.10
n -σ*	LP (1) N 18	1.921	BD*(1) C 8 - C 16	0.036	42.76	0.87	0.09
			BD*(1) C 16 - H 17	0.022	16.74	0.80	0.05
			BD*(1) N 19 - H 20	0.042	33.05	0.75	0.07
n -π*	LP (1) N 19	1.679	BD*(2) C 16 - N 18	0.212	102.42	0.30	0.08
			BD*(1) C 21 - O 29	0.021	5.40	0.87	0.03
			BD*(2) C 21 - O 29	0.274	170.41	0.33	0.10
n -σ*	LP (1) N 32	1.917	BD*(1) C 22 - C 24	0.033	39.46	0.89	0.08
			BD*(1) C 24 - H 27	0.023	16.57	0.78	0.05
			BD*(1) C 25 - C 23	0.026	8.16	4.18	0.08
			BD*(1) C 30 - H 31	0.023	17.11	0.77	0.05
n -σ*	LP (1) O 29	1.979	BD*(1) C 21 - C 22	0.066	8.24	1.12	0.04
n -σ*	LP (2) O 29	1.868	BD*(1) N 19 - C 21	0.073	99.66	0.68	0.12
			BD*(1) C 21 - C 22	0.066	73.35	0.68	0.10
			BD*(1) C 25 - C 23	0.026	6.90	4.10	0.08
π*-π*	BD*(2) C 1 - C 2	0.477	BD*(2) C 3 - C 4	0.301	1195.8	0.01	0.08
π*-π*	BD*(2) C 7 - C 8	0.349	BD*(2) C 1 - C 2	0.477	711.11	0.01	0.06
π*-σ*	BD*(2) C 21 - O 29	0.274	BD*(1) C 21 - O 29	0.021	18.24	0.54	0.11
π*-π*	BD*(2) C 30 - N 32	0.373	BD*(2) C 22 - C 24	0.328	604.96	0.02	0.08
			BD*(2) C 23 - C 25	0.287	714.04	0.02	0.08

[a] $E^{(2)}$ means energy of hyper conjugative interaction (stabilization energy).
[b] Energy difference between donor (i) and acceptor (j) nbo orbitals.
[c] F(i,j) is the Fock matrix element between i and j nbo orbitals.

HOMO–LUMO Analysis

The HOMO–LUMO plot of ICINH molecule is shown in Figure 4. In HOMO diagram, the colored portions indicate the prominent donor levels which contribute in the electronic transitions and similarly the LUMO diagram indicates the prominent acceptors level through colored shades which involve in the electronic transitions. Homo is localized in the indole and carbonyl group. The LUMO is located over the pyridine and hydrazone linkage. The molecule ICINH has lower energy gap and hence the probability of π-π* proton transition is highly possible in between HOMO and LUMO orbitals. The HOMO/LUMO energies are calculated using B3LYP/6-311++G(d,p) level.

DOI: 10.14302/issn.2377-2549.jndc-17-1459

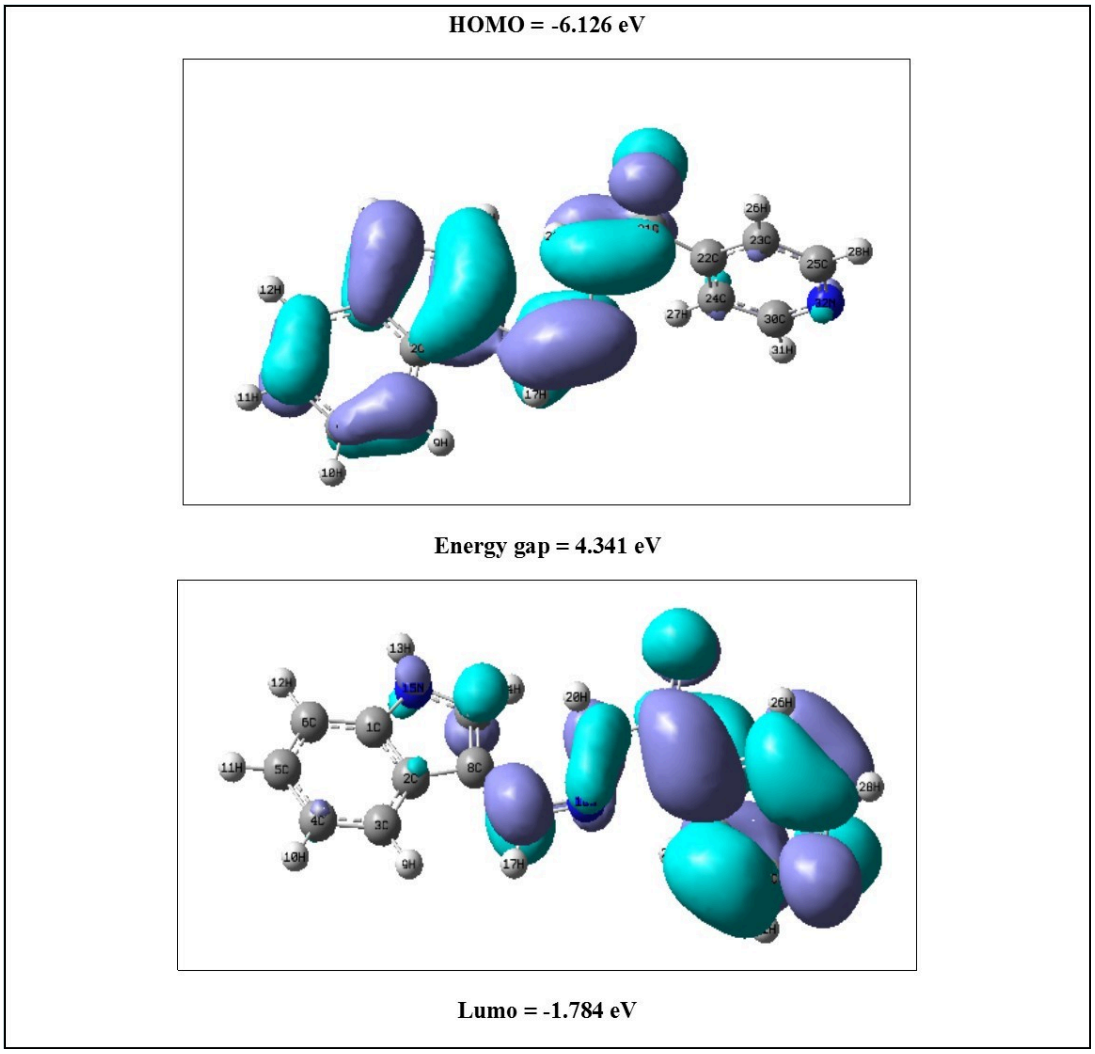


Figure 4. The frontier molecular orbitals of ICINH

By using HOMO and LUMO energy values of ICINH, the global chemical reactivity descriptors such as hardness (η), chemical potential (μ), softness (S), electronegativity (χ) and electrophilicity index (ω) have been calculated and are listed in Table 5. It can be expressed through HOMO and LUMO orbital energies as $I=-E_{HOMO}$ and $A=-E_{LOMO}$, the electron affinity I and Ionization potential A of title molecule ICINH are also calculated by using B3LYP/6-311++G(d,p) basis set. The calculated values of the softness, hardness, chemical potential, electronegativity and electrophilicity index, Homo, Lumo and energy gap of the molecule are: 4.341 eV, 3.954 eV, 3.954 eV and 1.801 eV, -6.125 eV, -1.784 eV and 4.341 eV, respectively. The soft molecule has small energy gap and hard molecule has large energy gap. In addition, the frontier molecular orbital energies are also calculated using the same basis set and are listed in Table 6.

 DOI: 10.14302/issn.2377-2549.jndc-17-1459

Table 5. The Physico-chemical properties of ICINH

Parameters	Values
HOMO	-6.125 eV
LUMO	-1.784 eV
Energy gap	4.341 eV
Ionization potential (IP)	6.125 eV
Electron affinity (EA)	1.784 eV
Electrophilicity Index (ω)	1.801
Chemical Potential (μ)	3.954
Electronegativity (χ)	-3.954
Hardness (η)	-4.341
Softness (S)	8.682

UV-Vis Spectra

The UV absorption spectrum for ICINH is recorded in the range 200-800 nm. All the structures allow strong π-π* and σ-σ* transition in the UV-Vis region with high extinction coefficients. The calculated results involving the vertical excitation energies, oscillator strength (f) and wavelength are carried out and compared with measured experimental wavelength. Typically, according to Frank-Condon principle, the maximum absorption peaks (λ_{max}) in a UV-Vis spectrum correspond to vertical excitation. The λ_{max} of ICINH molecule are calculated using TD-DFT/6-311++G(d,p) basis set. It is evident from the Table 7, the possible π-π* transitions, with absorption maximum at 413.14, 389.2, 357.32 nm, belong to gas phase and the oscillator strength for respective transitions are 0.0009, 0.0136 and 0.0296, respectively. The calculated absorption maxima has been found to be 357.32 nm which moderately

Table 6. The frontier molecular orbitals of ICINH

Occupancy	Orbital energies(a.u)	Orbital energies(eV)	Kinetic energies(a.u)
O_{52}	-0.269	-7.319	1.267
O_{53}	-0.267	-7.265	1.605
O_{54}	-0.262	-7.129	1.871
O_{55}	-0.254	-6. 911	1.250
O_{56}	-0.228	-6.203	1.576
V_{57}	-0.071	-1.931	1.664
V_{58}	-0.055	-1.496	1.519
V_{59}	-0.034	0. 925	1.367
V_{60}	0.025	0.680	0.381
V_{61}	0.023	0.625	1.250

DOI: 10.14302/issn.2377-2549.jndc-17-1459

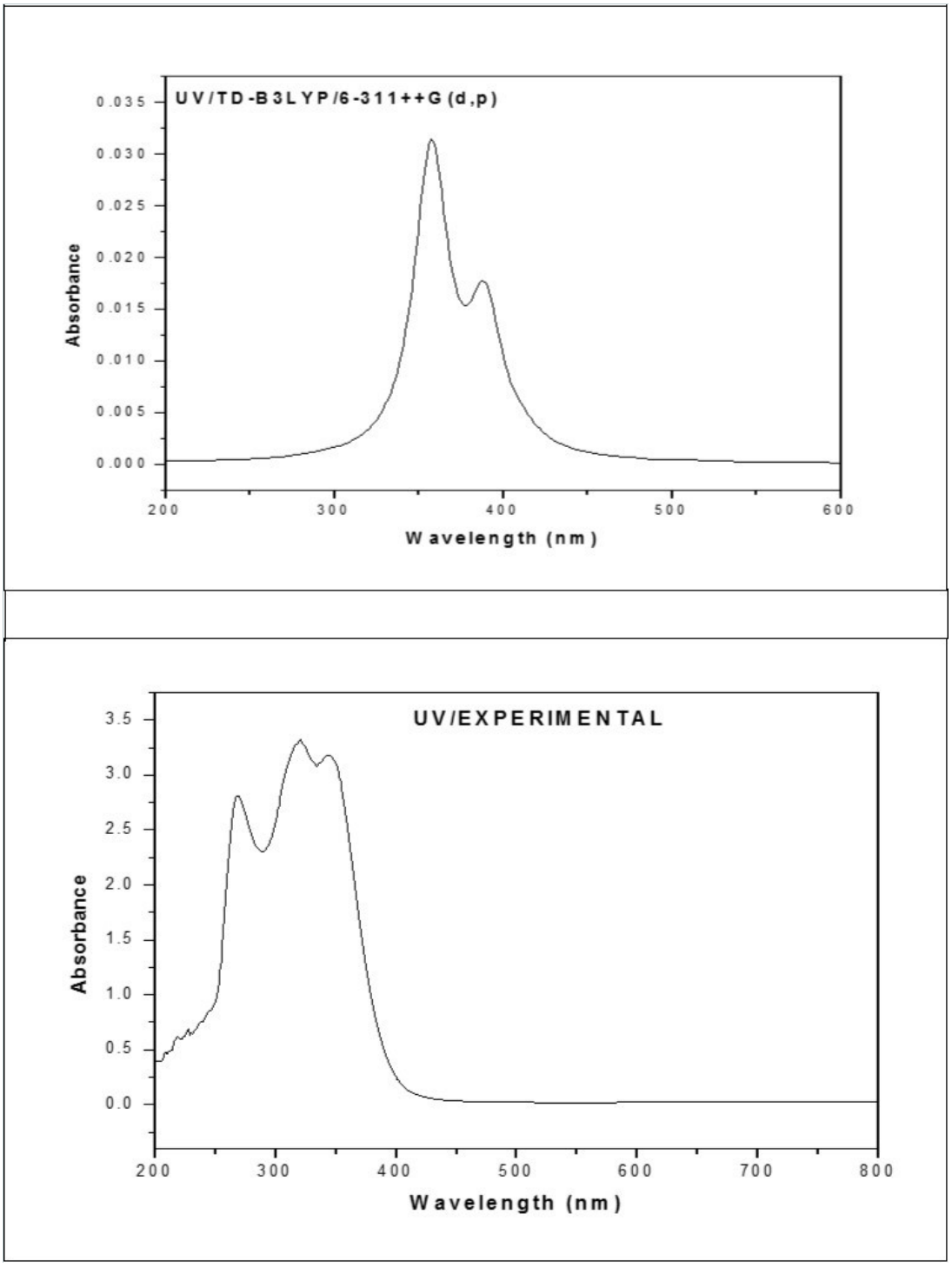


Figure 5. The combined theoretical and experimental UV-Visible spectra of ICINH

coincides with the experimental value 342.42 nm. The combined theoretical and experimental UV-Vis absorption spectra are shown in Figure 5.

Molecular electrostatic potential

In the present study, MEP surface map of ICINH is calculated using B3LYP/6-311++G(d,p) basis set and illustrated in Figure 6. The MEP is a plot of electrostatic potential map onto the constant ED surface. In the majority of the MEPs, the maximum negative region is the preferred site for electrophilic attack and the maximum positive region is the preferred site for nucleophilic attack. The importance of MEPs lies in the fact that it simultaneously displays molecular size, shape as well as positive, negative and neutral electrostatic potential regions in terms of colour scheme (Figure 6) and is very useful in research

Table 7. The electronic transition of ICINH

Calculated at B3LYP/6-311++G(d,p)	Oscillator strength	Calculated Band gap (ev/nm)	Experimental Band gap (ev/nm)	Type
Excited State-1	Singlet-A (f=0.0009)	3.0010 eV/413.14 nm		
69 -> 70	0.6908			
Excited State-2	Singlet-A (f=0.0136)	3.1849 eV/389.29 nm		
66 -> 70	-0.1059			
68 -> 70	0.6587			
68 -> 71	0.1308			
Excited State-3	Singlet-A (f=0.0296)	3.4698 eV/357.32 nm	342.42	π-π*
66 -> 70	0.1243			
66 -> 71	0.1564			
68 -> 70	-0.1275			
68 -> 71	0.4689			
69 -> 71	-0.4067			

of molecular structure with its physiochemical property relationship [26], [27]. The color scheme for the MEP surface is as follows: red for electron rich, partially negative charge: blue corresponds to electron deficient, partially positive charge: green for neutral, respectively [28], [29]. The electrostatic potential increases in the order of red<orange<yellow<green<blue. The color code of the map range between -9.185 e^{-2} (deepest red) to 9.185 e^{-2} (deepest blue). It is seen from the MEP map of the title molecule, the regions having the negative potential over the electronegative atom (oxygen atom), and the regions having the positive potential over all the hydrogen atoms in indole ring. The oxygen atom indicates the strong repulsion with other atom. These two ends of the molecule which are positively and negatively charged are prone to electrophilic and electrophobic reactions with other molecules.

Mulliken Atomic Charges

It is well known that the atomic charges are very much dependent on how the atoms are defined. It also plays an important role in the application of quantum chemical calculation to molecular system because atomic charges affect the dipole moment, molecular polarizability, electronic structure and a

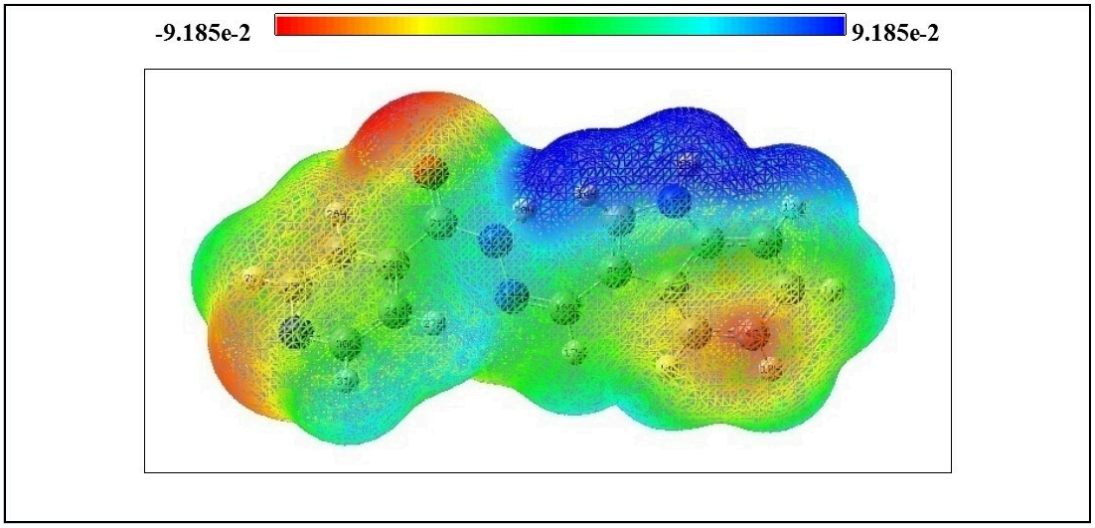


Figure 6. The molecular electrostatic potential map of ICINH

DOI: 10.14302/issn.2377-2549.jndc-17-1459

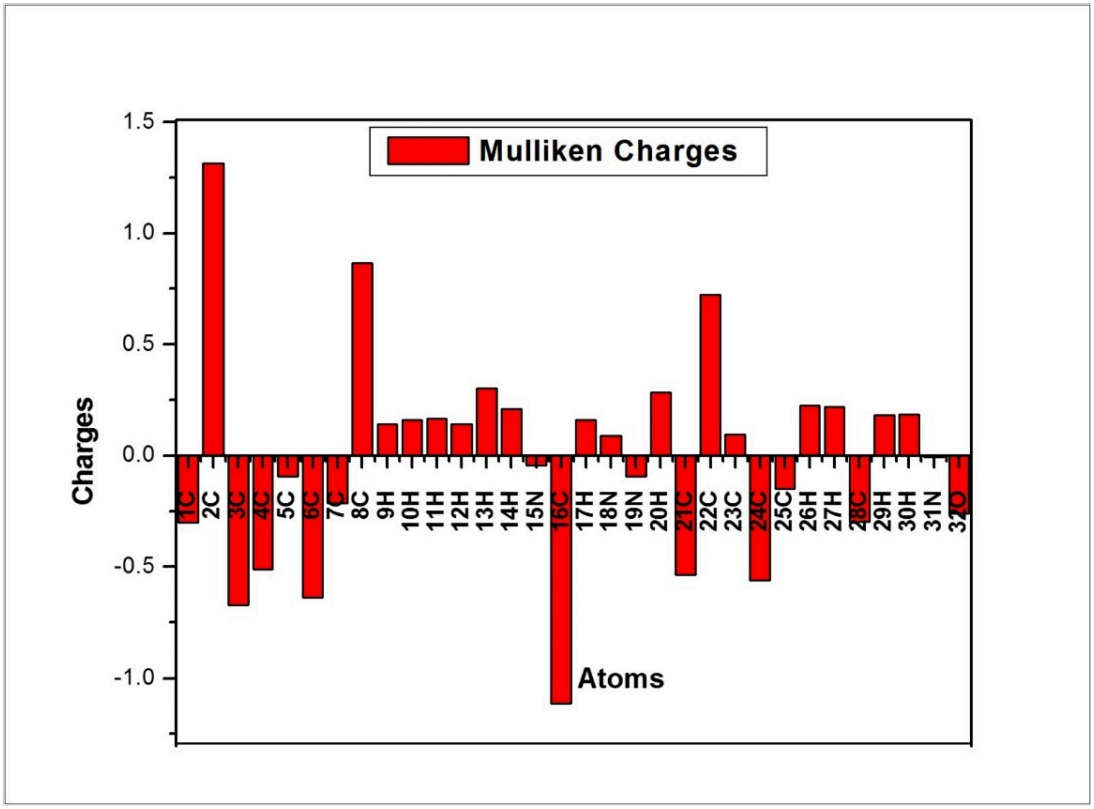


Figure 7. The Mulliken atomic charges of ICINH

lot of properties of molecular systems. The mulliken charges calculated at B3LYP/6-311++G(d,p) basis set for the molecule under study are given in Table 8. The mulliken atomic charges plot for ICINH is shown in Figure 7.

The C_2 atom has high positive charge which is due to the indole group. Similarly the C_{16} atom has high negative charge due to the attachment of C_{16}=N_{18} group. All the hydrogen atoms have positive charge.

Thermodynamic Properties

On the basis of vibrational analysis, the standard statistical thermodynamic functions: heat capacity (C), entropy (S) and enthalpy changes (H) for the title molecule are obtained from the theoretical harmonic frequencies and are listed in Table 9. From Table 10, it can be observed that these thermodynamic functions are increasing with temperature ranging from 100 to 1000 K. The obvious reason for this is almost linear increase, and this is due to the increase in internal energy of the molecule in accordance with kinetic theory of gases due to the fact that the molecular vibrational intensities increase with temperature [30]. The correlation equations between heat capacities, entropies, enthalpy changes and temperatures are fitted by quadratic formulas and the corresponding fitting factors (R^2) for these thermodynamic properties are 0.99905, 0.9994 and 0.99998, respectively and the correlation graphics are shown in Figure 8.

 DOI: 10.14302/issn.2377-2549.jndc-17-1459

Table 8. The Mulliken atomic charges of ICINH

Atoms	Charges	Atoms	Charges
1C	-0.2987	17H	0.1624
2C	1.3144	18N	0.0896
3C	-0.6692	19N	-0.0922
4C	-0.5107	20H	0.2843
5C	-0.0917	21C	-0.5353
6C	-0.6358	22C	0.7243
7C	-0.2138	23C	0.0949
8C	0.8639	24C	-0.5605
9H	0.1424	25C	-0.1468
10H	0.1605	26H	0.2244
11H	0.1674	27H	0.2180
12H	0.1439	28C	-0.2971
13H	0.3039	29H	0.1812
14H	0.2100	30H	0.1860
15N	-0.0449	31N	-0.0054
16C	-1.1123	32O	-0.2591

Table 9. The calculated total energy (a.u), zero point vibrational energies (Kcal/mol), rotational constants (GHz) and entropy (cal/mol K^{-1}) for ICINH

Parameters	B3LYP/6-311++G(d,p)
Total Energies	-873.259
Zero-point Energy	154. 930 (Kcal/Mol)
Rotational constants (GHZ)	1.119
	0.128
	0.120
Entropy	
Total	131.409
Translational	42.613
Rotational	34.185
Vibrational	54.610

 DOI: 10.14302/issn.2377-2549.jndc-17-1459

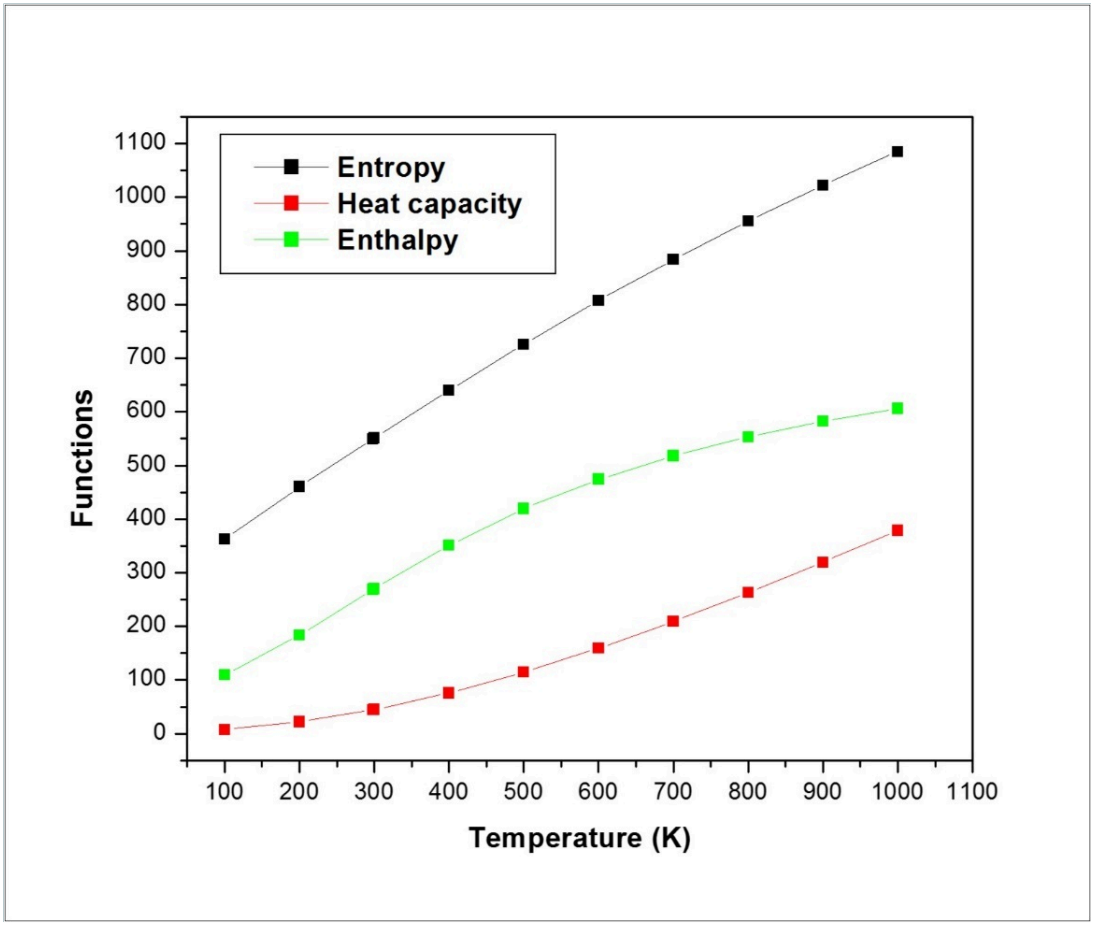


Figure 8. The thermodynamic properties of ICINH at different temperatures

They can be used to compute the other thermodynamic energies according to relationships of thermodynamic functions and estimate directions of chemical reactions according to the second law of

Table 10. Thermodynamic Properties of ICINH at different temperatures

T (K)	S (J/mol.K)	Cp (J/mol.K)	ddH (kJ/mol)
100.00	362.62	109.42	7.39
200.00	460.26	183.91	21.90
298.15	549.35	268.44	44.07
300.00	551.01	270.03	44.57
400.00	640.10	351.39	75.73
500.00	726.10	419.62	114.40
600.00	807.63	474.29	159.20
700.00	884.14	517.90	208.89
800.00	955.68	553.15	262.50
900.00	1022.55	582.09	319.31
1000.00	1085.17	606.19	378.76

thermodynamics in thermochemical field [31]. In this study all thermodynamic calculations are done in gas phase and they could not be used in solution.

$C^0_{p,m} = 6.76926 + 0.02858T + 2.52495x10^{-5} T^2$ ($R^2 = 0.99905$)

$S^0_m = 1.40875 + 0.00595T + 5.25468x10^{-5} T^2$ ($R^2 = 0.99998$)

$\Delta H^0_m = 4.06057 + 0.01714T + 1.51461x10^{-5} T^2$ ($R^2 = 0.9994$)

Conclusion

The FT-IR, FT-Raman and UV-Vis spectra of the compound ICINH had been recorded and analyzed. The detailed interpretations of the vibrational spectra had been carried out. The optimized geometrical parameters were calculated and compared with the reported XRD data. The vibrational assignments were further justified with the help of the PED analysis. The HOMO-LUMO energy gap indicated the stability and reactivity of the title compound. The good correlation between the UV-Vis absorption maxima and calculated electronic absorption maxima was found. The donor-acceptor interaction, as obtained from NBO analysis, could fairly explain the decrease of occupancies of σ bonding orbital and the increase of occupancy of π* anti-bonding orbitals. In addition, mulliken atomic charges, MEP, Thermodynamic parameters, first order hyperpolarizabilities and dipole moment of the title compound were also calculated.

Competing Interests

The authors have declared that no competing interests exist.

References

1. Ozisik H, Saglam S, Bayari S H. *Sturct. Chem*. 2009;19:41–50.
2. Hidgon J V, Delage B W, Dashwood R H. *Pharmacol. Res*. 2007;55(3):224.
3. Billes F, Podea P V, Mohammed-Ziegler I, Tosa M, Mikosch H, Irimie D F. *Spectrochim. Acta A*. 2009;74:1031–1045.
4. Taiz L, Zeiger E. *Plant Physiology*. second ed. Massachusetts: Sinauer Associates, Inc; 1998.
5. Carney J R, Timothy S Z. *J Phys. Chem. A*. 2004;104:8677–8688.
6. Vasantha Kumar V, Gouda S L, Laxmikanth Rao J. Ab initio and density functional theory studies on vibrational spectra of 3-hydroxy-3-(2-methyl-1H-indol-3-yl)indolin-2-one. *Spectrochimica Acta Part A: Molecular and Biomolecular Spectroscopy*. 2013;103:304–310. https://doi.org/10.1016/j.saa.2012.10.023
7. Saleem H, Subashchandrabose S, Erdogduc Y, Thanikachalam V, Jayabharathi J. FT-IR, FT-Raman spectral and conformational studies on (E)-2-(2-hydroxybenzylidenamino)-3-(1H-indol-3yl) propionic acid. *Spectrochimica Acta Part A: Molecular and Biomolecular Spectroscopy*. 2013;101:91–99. https://doi.org/10.1016/j.saa.2012.09.023
8. Ramesh Babu N, Subashchandrabose S, Padusha M Syed Ali, Saleem H, Manivannan V, Erdog˘du Y. Synthesis and structural characterization of (E)-N0-((Pyridin-2-yl)methylene) benzohydrazide by X-ray diffraction, FT-IR, FT-Raman and DFT methods. *Journal of Molecular Structure*. 2014;1072:84–93. https://doi.org/10.1016/j.molstruc.2014.04.060
9. Lissoni P, Bucovec R, Bonfonti A, Giani L, Mandelli A, Roselli M G, Rovelli F, Fumapalli L. *J. Pineal Res*. 2001;30(2):123. Parr R G, Yang W. *Density Functional Theory of Atoms and molecules*. Oxford, New York; 1989.
10. Jones R O, Gunnarson O. *Rev. Mod. Phys*. 1989;61:689–746.
11. Ziegler T. *Chem. Rev*. 1991;91:651–667.
12. Kohn W, Sham L J. *Phys. Rev.* 1965;146:A1133–A1138.
13. James C, Pettit G R, Nielsen O F, Jayakumar V S, Joe T H. *Spectrochimm. Acta A*. 2008;70:1208–1216.
14. Babu Dickson, Gachumale S, Sambandam A, Airody Vasudeva A. New D-p-A Type indole based chromoogens for DSSC: Design Synthesis and Performance studies. *Dyes and Pig*. 2015;112:183–191. https://doi.org/10.1016/j.dyepig.2014.07.006

15. Hassan M, Badawi, Former W. analysis of the molecular Stutucture and vibrational spectra of the title indole based analgesic drug indomethacin. *Spectrochim. Acta A: Mol. Biomol. Spectrosc*. 2014;123:447–454.
16. Bikas R, Sattarri F, Notash B. *Acta Cryst. E*. 2012;68:M132–M133.
17. Rauhut G, Pulay P. Transferable Scaling Factors for Density Functional Derived Vibrational Force Fields. *J.Phys.Chem*. 1995;99:3093–3100. https://doi.org/10.1021/j100010a019
18. Krishnakumar V, Ramasamy R. *Indian J Pure and Appl. Phys*. 2002;40:252.
19. George W O, Mcintyre P S. *Infrared Spectroscopy*. London: John Wiley and Sons; 1987.
20. Bellamy L J. *The infrared spectra of complex molecules*. New York: John Wiley; 1959.
21. Karabacak Mehmet. *J. Mol. Struct*. 2009;919:215–222.
22. Silverstein M, Clayton Basseler G, Morill C. *Spectrometric Identification of Organic Compounds*. New York: Wiley; 1981.
23. Ramalingam S, Periandy S, Narayanan B, Mohan S. *Spectrochim. Acta A*. 2010;76:84–92.
24. Nikitina A N, Yakovlev L P, Fedotov N S, Mikhailov B M. *Zhurnal Prikladnoi spektroskopii*. 1967;6(2):232–238.
25. Sun Y X, Hao Q L, Wei W X, Yu Z X, Lu L D, Wang X, Wang Y S. *J.Mol.Struct. (Therochem)*. 2009;904:74.
26. Murray J S, Sen K. *Molecular Electrostatic Potentials, Concepts and Applications*. Amsterdam: Elsevier; 1996.
27. Scrocco E, Tomasi J. Lowdin P, Ed. *Advances in Quantum Chemistry*. New York: Academic Press; 1978.
28. Roohi H, Nowroozi A R, Anjomshoa E. *Compt. Theor. Chem*. 2011;965:211–220.
29. Munshi P, Guru Row TN. *Acta Cryst.B*. 2006;62:612–626.
30. Bevan Ott J, Boerio-Goates J. Calculations from statistical thermodynamics, 588 Academic Press. 2000:589.
31. Zhang R, Dub B, Sun G, Sun Y. *Spectrochim. Acta A*. 2010;75:1115–1124.

Publisher's Note

All claims, opinions, data, and conclusions expressed in this article are solely those of the author(s) and contributor(s), and do not necessarily represent those of Open Access Pub, the journal, its editors, or reviewers. Open Access Pub does not guarantee or endorse any product, method, instruction, or claim discussed in the article, and disclaims responsibility for any injury to people or property resulting from ideas, methods, instructions, or products referred to in the content.